

Harnessing Chemical Exchange: ^{19}F Magnetic Resonance OFF/ON Zinc Sensing with A Tm(III) Complex

Meng Yu, Da Xie, Rahul T. Kadakia, Weiran Wang, Emily L. Que*
Department of Chemistry, University of Texas at Austin, Austin, TX 78712, United States

Materials and Methods	S2
Synthetic Methods	S3
Scheme S1. Synthesis of Tm-PFZ-1 , Yb-PFZ-1 , and Eu-PFZ-1	S3
Figure S1. HPLC trace of Tm-PFZ-1 at 254 nm detection	S5
Figure S2. High resolution mass spectrum of Tm-PFZ-1	S6
Figure S3. HPLC trace of Yb-PFZ-1 at 254 nm detection	S6
Figure S4. High resolution mass spectrum of Yb-PFZ-1	S7
Figure S5. HPLC trace of Eu-PFZ-1 at 254 nm detection	S7
Figure S6. High resolution mass spectrum of Eu-PFZ-1	S8
Figure S7. Illustration of structural isomerization	S8
Figure S8. ^{19}F NMR spectra of Yb-PFZ-1 and Eu-PFZ-1 in buffer after adding 1 equiv. Zn^{2+}	S9
Figure S9. ^{19}F NMR spectra of Gd-PFZ-1 , Tb-PFZ-1 , Dy-PFZ-1 , Er-PFZ-1 , and Ho-PFZ-1 in buffer after adding 1 equiv. Zn^{2+}	S10
Figure S10. ^{19}F NMR titration of Tm-PFZ-1 with Zn^{2+}	S11
Figure S11. Job's plot of Tm-PFZ-1 with Zn(II) using NMR	S11
Figure S12. ^{19}F NMR spectra after repetitive addition of Zn^{2+} and EDTA to Tm-PFZ-1	S12
Figure S13. Luminescence spectra of Eu-PFZ-1 in the presence of Zn(II)	S13
Figure S14. ^{19}F NMR spectra of Tm-PFZ-1 in presence of $\text{Ca}^{2+}/\text{Mg}^{2+}$ with or without Zn^{2+}	S14
Figure S15. ^{19}F NMR spectrum of Tm-PFZ-1 in presence of Cu^{2+}	S15
Figure S16. ^{19}F NMR spectra of Tm-PFZ-1 in presence of lactate, HCO_3^- or BSA and Zn^{2+}	S16
Figure S17. UV-vis spectrum of 0.2 mM Eu-PFZ-1 in 50 mM HEPES buffer	S17
Figure S18. Fitting of luminescence titration data of Eu-PFZ-1 into a 1:1 binding model	S17
Figure S19. ^1H NMR spectra of Eu-PFZ-1 in D_2O and after adding Zn^{2+}	S18
Table S1. Peak width at half maximum of Yb-PFZ-1 from 10-85 °C	S18
Table S2. Peak width at half maximum of Yb-PFZ-1 with Zn^{2+} from 10-85 °C	S18
Figure S20. Limit of detection measurement of Tm-PFZ-1 by ^{19}F MRI	S19
Figure S21. ^1H NMR spectrum of 3 in CDCl_3	S20
Figure S22. ^{19}F NMR spectrum of 3 in CDCl_3	S21
Figure S23. ^{13}C NMR spectrum of 3 in CDCl_3 .	S22
Figure S24. ^1H NMR spectrum of 5 in CDCl_3	S23
Figure S25. ^{19}F NMR spectrum of 5 in CDCl_3	S24
Figure S26. ^{13}C NMR spectrum of 5 in CDCl_3	S25
Figure S27. ^1H NMR spectrum of L in CD_3OD	S26
Figure S28. ^{19}F NMR spectrum of L in CD_3OD	S27
Figure S29. ^{13}C NMR spectrum of L in CD_3OD	S28
References	S28

Materials and Methods

Materials

Except where stated otherwise, all chemicals were purchased from Sigma-Aldrich and Fisher Scientific and used as received. 1,4,7,10-tetraazacyclododecane was purchased from Strem Chemicals. Deuterated solvents were purchased from Cambridge Isotope Laboratories. **1**^[1], NaOC(CF₃)₃^[2], **4**^[3] and **¹³Bu-DO3A**^[4] were synthesized according to modified literature procedures.

Instrumentation

All ¹H, ¹³C and ¹⁹F NMR spectra were recorded on a 400 MHz or 500 MHz Agilent NMR spectrometer; all reported resonances were referenced to internal standards. VT NMR experiments were performed on a 600 MHz Agilent VNMRs600 spectrometer. ¹⁹F NMR peaks were referenced versus 5-fluorocytosine. The accurate thulium complex concentration was determined using ICP-OES. T₁ relaxation time was determined using the inversion-recovery method and T₂ relaxation time was measured using the CPMG pulse sequence. Walk-up LC-MS and high-resolution Electrospray Ionization (ESI) mass spectral analyses were performed by the Mass Spectrometry Facility of the Department of Chemistry at UT Austin. Electrode-based pH measurements were carried out using a Thermo Scientific Orion 9110DJWP double junction pH electrode connected to a Sartorius PB-11 pH meter. Solid state infrared spectra were recorded on a Bruker Alpha spectrometer equipped with a diamond ATR crystal. UV/vis spectra were recorded on an Agilent Cary 6 UV/vis spectrometer. Luminescence measurements were performed by a Photon Technology International QM 4 spectrophotometer. MR images were collected on a Bruker BioSpin (Karlsruhe, Germany) Pharmascan 70/16 magnet with a BioSpec two-channel console and BGA-9s gradient coil in the Imaging Research Center at UT Austin.

Job's plot

A 2.85 mM stock solution of **Tm-PFZ-1** in 50 mM HEPES (pH=7.4, 0.1 M KNO₃) was prepared (concentration determined by ICP-OES). 500 μL samples containing different ratios (9:1, 8:2, 7:3, 6:4, 5:5, 4:6, 3:7, 2:8, 1:9) of **Tm-PFZ-1** and ZnSO₄ was then prepared while maintaining a constant total concentration of 2 mM ([**1**]+[Zn]). 1 mM 5-fluorocytosine was added to each sample as an internal ¹⁹F reference. ¹⁹F NMR spectra were collected for all the samples and the peak at -112.4 ppm was integrated based upon reference. The integrals were plotted versus mole fraction of Zn²⁺ to obtain Job's plot.

Response towards cations, anions and proteins

To 1 mM **Tm-PFZ-1** in 50 mM HEPES (pH=7.4, 0.1 M KNO₃) was added 1 mM MgCl₂ or CaCl₂ and ¹⁹F NMR was performed. No ¹⁹F NMR signal can be observed and 1 mM ZnSO₄ then added. Similarly, 1 mM CuSO₄ was added to **Tm-PFZ-1** and ¹⁹F NMR was recorded. The response of 1 mM **Tm-PFZ-1** towards 1 mM ZnSO₄ was also tested by ¹⁹F NMR in the presence of 2 mM citrate, 10 mM HCO₃⁻ or 5 mg/mL bovine serum albumin (BSA).

Determination of apparent dissociation constant with Zn²⁺ by luminescence measurements

50 μM **Eu-PFZ-1** in 50 mM HEPES (pH=7.4, 0.1 M KNO₃) was prepared. 0-2 Equiv. of Zn²⁺ was gradually added and the emission spectra were recorded at excitation wavelength of 265 nm. The emission intensity at 616 nm was plotted against the concentration of Zn²⁺ and fitted into a 1:1 binding mode using the following equation:

$$(F-F_0)/(F_{\max}-F_0) = [Zn^{2+}]/(K_d + [Zn^{2+}])$$

where F₀ is the luminescence intensity in the absence of Zn²⁺, F_{max} is the maximum luminescence intensity and [Zn²⁺] is the free Zn²⁺ concentration.

Decay of luminescence emission at 616 nm was fitted into a single exponential curve to obtain the luminescence lifetime of **Eu-PFZ-1** in H₂O or D₂O in the presence or absence of 1 equiv. Zn²⁺.

$$I = I_0 \exp(-t/\tau)$$

where I_0 and I are the luminescence intensities at the time $t = 0$ and time t , respectively, and τ is the luminescence emission lifetime. Lifetimes were obtained by monitoring the emission intensity at 616 nm ($\lambda_{\text{ex}} = 265$ nm). The inner-sphere water number (q) was calculated using the following equation:

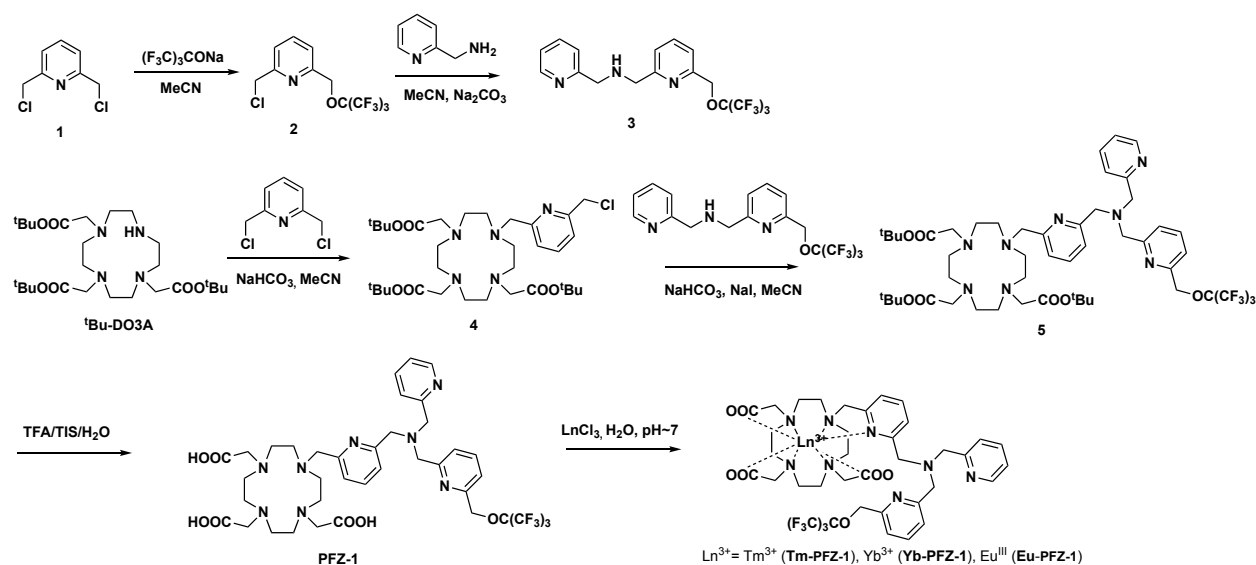
$$q = 1.11(1/\tau_{\text{H}_2\text{O}} - 1/\tau_{\text{D}_2\text{O}} - 0.31)$$

¹⁹F MRI Experiments

The magnetic resonance imaging experiments were performed on a Bruker BioSpin (Karlsruhe, Germany) Pharmascan 70/16 magnet with a BioSpec two-channel console and BGA-9s gradient coil. The RF coil was a quadrature single resonance tunable T/R coil (Doty Scientific, Inc., Columbia, South Carolina, USA) with a resonant frequency of 282.2 MHz to correspond to ¹⁹F at 7.0 T. Each element of the RF coil was tuned and matched with the samples loaded using a Morris frequency sweeper (Morris Instruments, Inc. Ottawa, Ontario, Canada) while the complementary element was terminated with the receive chain of the instrument. All prescan adjustments and imaging was performed using product sequences and methods in ParaVision 6.0.1 (Bruker, vide supra).

Solutions were imaged while contained in standard 600 μL Eppendorf tubes mounted in a 3 \times 3 grid by a custom holder produced on a Form 2 3D printer (FormLabs, Inc., Somerville, Massachusetts, USA). For limit of detection study, complexes were dissolved in 500 μL of 50 mM pH 7.4 HEPES buffer (0.1 M NaCl) at different concentrations with optimized RARE (Rapid Acquisition with Relaxation Enhancement) sequence parameters. *Zn²⁺ detection experiment*: 0-1.0 equiv. Zn²⁺ was added to 6 mM **Tm-PFZ-1** in 50 mM HEPES (pH=7.4, 0.1 M KNO₃) and fast spin-echo ¹⁹F MR imaging was conducted using Rapid Acquisition with Relaxation Enhancement (RARE) sequence. *Limit of detection experiment*: HEPES buffer solutions containing different concentrations of equivalent molar of **Tm-PFZ-1** and Zn²⁺ were prepared and fast spin-echo ¹⁹F MR imaging was performed. *Low Zn²⁺ detection*: To 200 μM Zn²⁺ in 50 mM HEPES (pH=7.4, 0.1 M KNO₃) was introduced 200 μM **Tm-PFZ-1** and fast spin-echo ¹⁹F MR imaging was performed. RARE sequence parameters: TE (Echo Time) = 1.55 ms, TR (Repetition Time) = 100 ms, NA (Number of Averages) = 3000, FA (Flip Angle) = 90°, rare factor = 8, BW (Bandwidth) = 7.5 kHz, matrix size = 32 x 32, FOV (Field of View) = 20 x 20 mm, ST (Slice Thickness) = 50 mm, scan time = 20 min.

Synthetic Methods



Scheme S1. Synthetic route for ligand and complexes **Tm-PFZ-1**, **Yb-PFZ-1**, and **Eu-PFZ-1**.

2

1 (1.36 g, 7.72 mmol) and NaI (58 mg, 0.388 mmol) were dissolved in 30 mL dry MeCN under N₂. The solution was heated to 80 °C and a suspension of NaOC(CF₃)₃ (1.0 g, 3.88 mmol) in 50 mL MeCN was added slowly. The resultant suspension was kept under 80 °C for 16 h and cooled down to RT. After filtration, the filtrate was evaporated and subjected to silica gel column. Use Dichloromethane/hexanes (3% to 5%) to remove the di-substituted product and ethyl acetate/hexanes (3% to 4%) to get the product as a colorless oil (~1.0 g, 69% yield). ¹H NMR (500 MHz, Chloroform-*d*) δ 7.72 (t, *J* = 7.8 Hz, 1H), 7.35 (dd, *J* = 12.4, 7.6 Hz, 2H), 5.11 (s, 2H), 4.56 (s, 2H). ¹⁹F NMR (471 MHz, CDCl₃) δ -70.36. ¹³C NMR (126 MHz, CDCl₃) δ 156.13, 155.01, 138.12, 122.16, 119.79, 71.23, 46.33. LRMS (ESI⁺): Calcd for [M+H]⁺ (C₁₁H₈ClF₉NO) 376.0, found 376.0.

3

2-Picolylamine (480 mg, 4.44 mmol) and anhydrous Na₂CO₃ (471 mg, 4.44 mmol) were combined in a 100 mL round bottom flask and dissolved with 20 mL anhydrous MeCN. The suspension was stirred at 40 °C degree for half an hour. Compound **2** (834 mg, 2.22 mmol) in 10 mL MeCN was added dropwise to the solution and the mixture was stirred at 65 °C for 16 h. The solution was then filtered and evaporated. The crude was purified by reverse phase chromatography using MeCN/H₂O as eluent (contain 0.1% TFA, product came out at 40% MeCN) to yield about 740 mg light brown oil product as a TFA salt. ¹H NMR (500 MHz, Chloroform-*d*) δ 8.61 (d, *J* = 5.2 Hz, 1H), 8.01 (td, *J* = 7.8, 1.6 Hz, 1H), 7.79 (t, *J* = 7.8 Hz, 1H), 7.71 (d, *J* = 7.8 Hz, 1H), 7.55 (dd, *J* = 7.7, 5.3 Hz, 1H), 7.45 (d, *J* = 7.8 Hz, 1H), 7.28 (d, *J* = 7.6 Hz, 1H), 5.12 (s, 2H), 4.64 (s, 2H), 4.49 (s, 2H). ¹⁹F NMR (471 MHz, CDCl₃) δ -70.64, -76.24 (TFA). ¹³C NMR (126 MHz, CDCl₃) δ 155.19, 149.53, 148.21, 146.58, 141.28, 138.77, 125.83, 125.49, 122.30, 121.00, 70.72, 50.53, 49.16. LRMS (ESI⁺): Calcd for [M+H]⁺ (C₁₇H₁₅F₉N₃O) 448.1, found 448.1.

5

3 (740 mg, ~0.94 mmol), **4** (616 mg, 0.94 mmol), NaI (70.6 mg, 0.47 mmol) and NaHCO₃ (395 mg, 4.70 mmol) were combined and dissolved in 20 mL anhydrous MeCN. The suspension was stirred at 65 °C for 40 h and filtered. The filtrate was evaporated and purified by reverse phase chromatography using MeCN/H₂O as eluent (contain 0.1% HCOOH, product came out at 60% MeCN) to yield about 700 mg light brown oil as the product. ¹H NMR (500 MHz, Chloroform-*d*) δ 8.47 (d, *J* = 4.8 Hz, 1H), 7.78 – 7.42 (m, 7H), 7.28 (d, *J* = 7.7 Hz, 1H), 7.12 (t, *J* = 6.3 Hz, 1H), 5.10 (s, 2H), 4.47 (s, 2H), 3.81 (d, *J* = 8.2 Hz, 6H), 3.51 (s, 2H), 3.31 (d, *J* = 13.5 Hz, 8H), 3.02 (d, *J* = 5.4 Hz, 4H), 2.83 (s, 8H), 1.39 (d, *J* = 17.9 Hz, 27H). ¹⁹F NMR (471 MHz, CDCl₃) δ -70.33. ¹³C NMR (126 MHz, CDCl₃) δ 170.44, 169.93, 166.97, 159.49, 158.91, 158.87, 154.29, 149.03, 148.98, 137.73, 137.63, 136.59, 122.80, 122.50, 122.19, 122.15, 121.44, 119.04, 81.72, 81.57, 71.48, 60.18, 60.13, 60.09, 56.60, 56.15, 52.80, 51.74, 50.86, 49.11, 28.03. LRMS (ESI⁺): Calcd for [M+H]⁺ (C₃₈H₄₆F₉N₈O₇) 1066.1, found 1066.1.

PFZ-1

700 mg **5** was dissolved in 5 mL TFA/triisopropylsilane/H₂O (95/2.5/2.5, v/v/v) using an ice bath. The solution was stirred for 16 h and then solvent was removed using a N₂ flow. The crude was purified by reverse phase chromatography using MeCN/H₂O as eluent (contain 0.1% HCOOH, product came out at 30% MeCN) to yield about 400 mg white solid as the product. ¹H NMR (500 MHz, Methanol-*d*₄) δ 8.49 (d, *J* = 4.8 Hz, 1H), 7.95 – 7.75 (m, 3H), 7.71 (d, *J* = 7.9 Hz, 1H), 7.65 (t, *J* = 7.6 Hz, 2H), 7.57 (d, *J* = 7.7 Hz, 1H), 7.40 (d, *J* = 7.7 Hz, 1H), 7.34 (dd, *J* = 7.5, 5.1 Hz, 1H), 5.20 (s, 2H), 4.23 – 3.96 (m, 8H), 3.84 – 3.25 (m, 14H), 3.10 (d, *J* = 31.9 Hz, 8H). ¹⁹F NMR (471 MHz, CDCl₃) δ -71.51. ¹³C NMR (126 MHz, MeOD) δ 165.43, 157.53, 157.16, 157.10, 153.88, 147.85, 139.15, 138.05, 137.78, 124.12, 124.01, 123.39, 122.89, 122.81, 121.54, 120.25, 119.21, 71.70, 59.20, 59.11, 58.96, 57.66, 55.99, 53.89, 51.06, 50.18, 48.67, 48.32, 27.47. LRMS (ESI⁺): Calcd for [M+H]⁺ (C₅₀H₇₀F₉N₈O₇) 897.3, found 897.3.

Tm-PFZ-1

L (50 mg, 0.055 mmol) was dissolved in 5 mL H₂O and the pH was adjusted to 7 with 1 N NaOH solution. Thulium(III) chloride (24.5 mg, 0.061 mmol) in 1 mL H₂O was added in one portion. The solution was readjusted to pH 7 and stirred for 3 h followed by filtration and lyophilization. The crude was purified by reverse phase chromatography using 50 mM ammonium acetate buffer (pH~6.5) and MeCN (contain 5% ammonium acetate buffer) as eluent (product came out at 60% MeCN) to yield about 60 mg white solid as the product. HRMS (ESI⁺): Calcd for [M+H]⁺ (C₃₈H₄₄F₉N₈O₇Tm) 1063.2448, found 1063.2446.

Yb-PFZ-1

L (12.9 mg, 0.014 mmol) was dissolved in 3 mL H₂O and the pH was adjusted to 7 with 1 N NaOH solution. Ytterbium(III) chloride hexahydrate (6.1 mg, 0.016 mmol) was added in one portion. The solution was readjusted to pH 7 and stirred for 2 h followed by filtration and purification. The crude was purified by reverse phase chromatography using 50 mM ammonium acetate buffer (pH~6.5) and MeCN (contain 5% ammonium acetate buffer) as eluent (product came out at 60% MeCN) to yield about 12 mg white solid as the product. HRMS (ESI⁺): Calcd for [M+H]⁺ (C₃₈H₄₄F₉N₈O₇Yb) 1068.2500, found 1068.2480.

Eu-PFZ-1

L (17.8 mg, 0.020 mmol) was dissolved in 5 mL H₂O and the pH was adjusted to 7 with 1 N NaOH solution. Europium(III) chloride hexahydrate (8.0 mg, 0.022 mmol) in 1 mL H₂O was added in one portion. The solution was readjusted to pH 7 and stirred for 3 h followed by filtration and lyophilization. The crude was purified by reverse phase chromatography using 50 mM ammonium acetate buffer (pH~6.5) and MeCN (contain 5% ammonium acetate buffer) as eluent (product came out at 60% MeCN) to yield about 18 mg white solid as the product. HRMS (ESI⁺): Calcd for [M+H]⁺ (C₃₈H₄₄F₉N₈O₇Eu) 1045.2304, found 1045.2300.

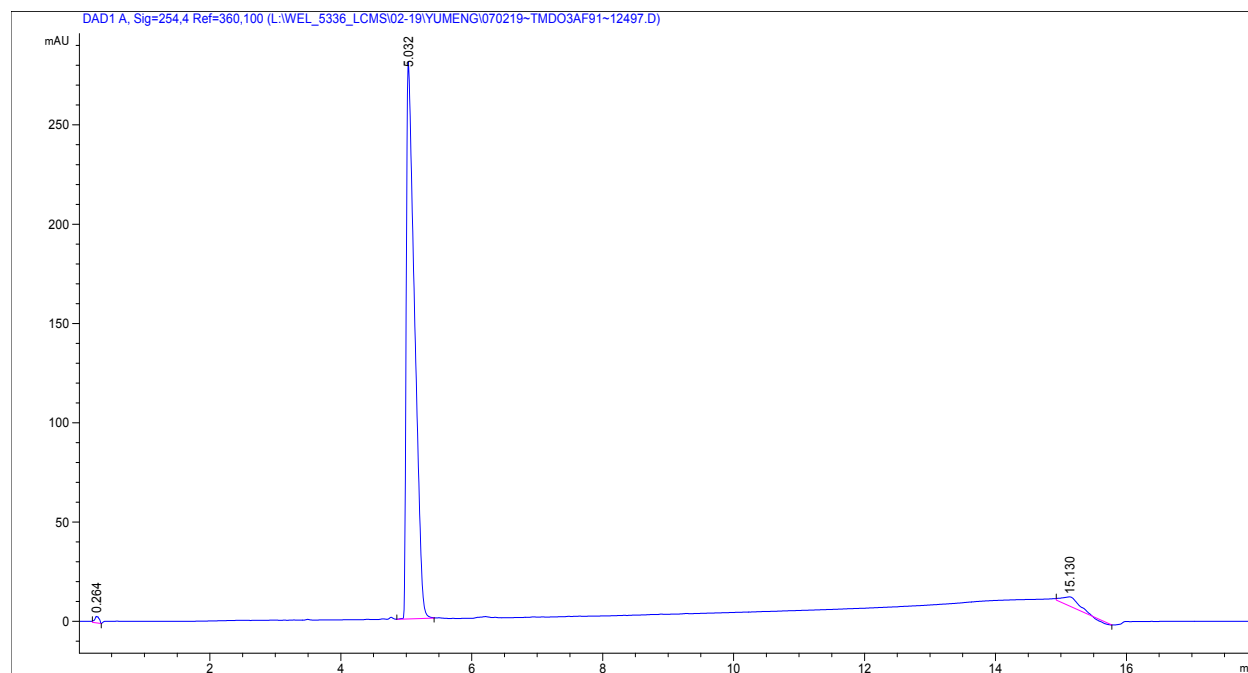
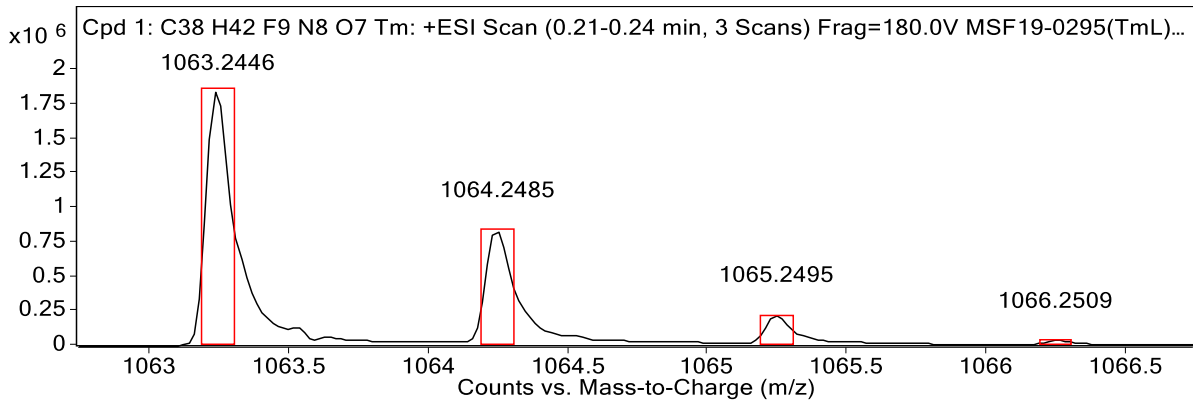


Figure S1. HPLC trace of **Tm-PFZ-1** at 254 nm detection.



MS Spectrum Peak List

Obs. m/z	Calc. m/z	Charge	Abundance	Formula	Ion Species	Tgt Mass Error (ppm)
1063.2446	1063.2448	1	1856645	C38H42F9N8O7Tm	(M+H)+	0.12
1064.2485	1064.2477	1	836382	C38H42F9N8O7Tm	(M+H)+	-0.69
1065.2495	1065.2505	1	220422	C38H42F9N8O7Tm	(M+H)+	0.89
1066.2509	1066.2531	1	32355	C38H42F9N8O7Tm	(M+H)+	2.13
1067.2265	1067.2557	1	8867	C38H42F9N8O7Tm	(M+H)+	27.34

--- End Of Report ---

Figure S2. High resolution mass spectrum of **Tm-PFZ-1**.

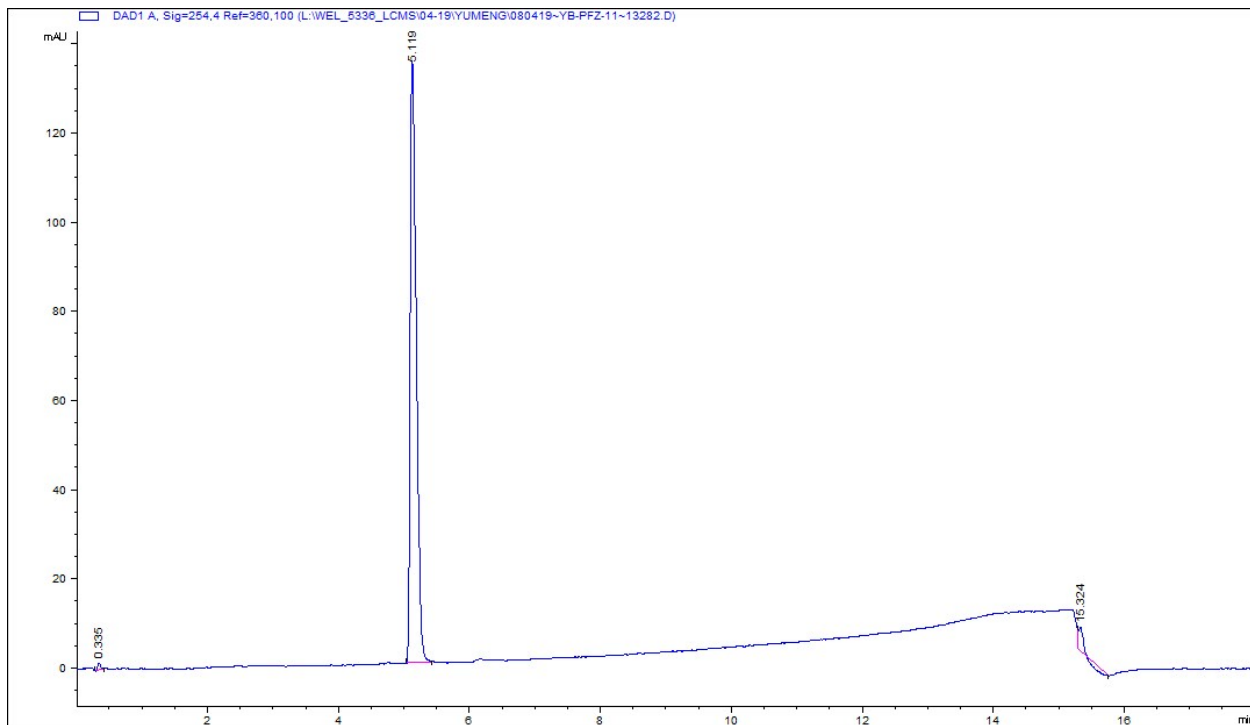
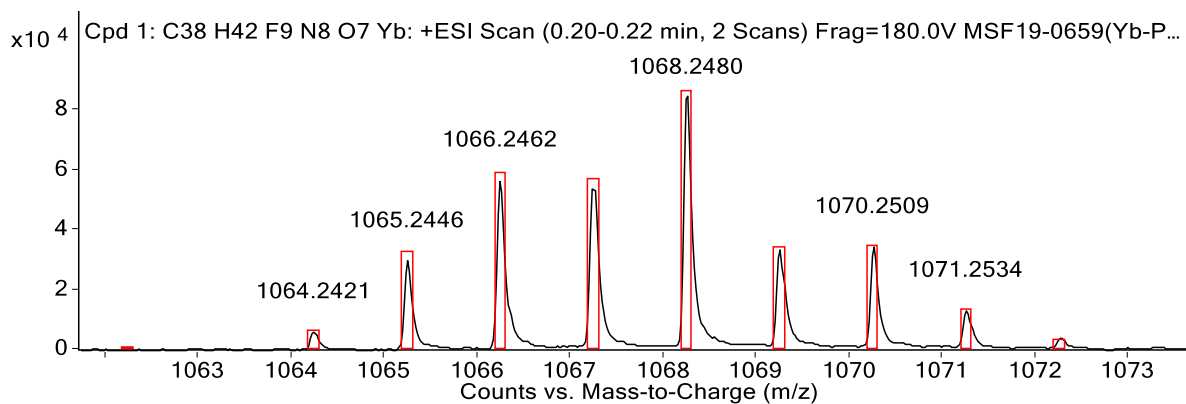


Figure S3. HPLC trace of **Yb-PFZ-1** at 254 nm detection.



MS Spectrum Peak List

Obs. m/z	Calc. m/z	Charge	Abundance	Formula	Ion Species	Tgt Mass Error (ppm)
365.1060			320787			
1062.2376	1062.2444	1	119	C ₃₈ H ₄₂ F ₉ N ₈ O ₇ Yb	(M+H) ⁺	6.43
1064.2421	1064.2453	1	6061	C ₃₈ H ₄₂ F ₉ N ₈ O ₇ Yb	(M+H) ⁺	3.02
1065.2446	1065.2470	1	29794	C ₃₈ H ₄₂ F ₉ N ₈ O ₇ Yb	(M+H) ⁺	2.28
1066.2462	1066.2476	1	56797	C ₃₈ H ₄₂ F ₉ N ₈ O ₇ Yb	(M+H) ⁺	1.38
1067.2475	1067.2494	1	55524	C ₃₈ H ₄₂ F ₉ N ₈ O ₇ Yb	(M+H) ⁺	1.8
1068.2480	1068.2500	1	86257	C ₃₈ H ₄₂ F ₉ N ₈ O ₇ Yb	(M+H) ⁺	1.92
1069.2511	1069.2527	1	33351	C ₃₈ H ₄₂ F ₉ N ₈ O ₇ Yb	(M+H) ⁺	1.48
1070.2509	1070.2537	1	34552	C ₃₈ H ₄₂ F ₉ N ₈ O ₇ Yb	(M+H) ⁺	2.59
1071.2534	1071.2563	1	13257	C ₃₈ H ₄₂ F ₉ N ₈ O ₇ Yb	(M+H) ⁺	2.69

Figure S4. High resolution mass spectrum of **Yb-PFZ-1**.

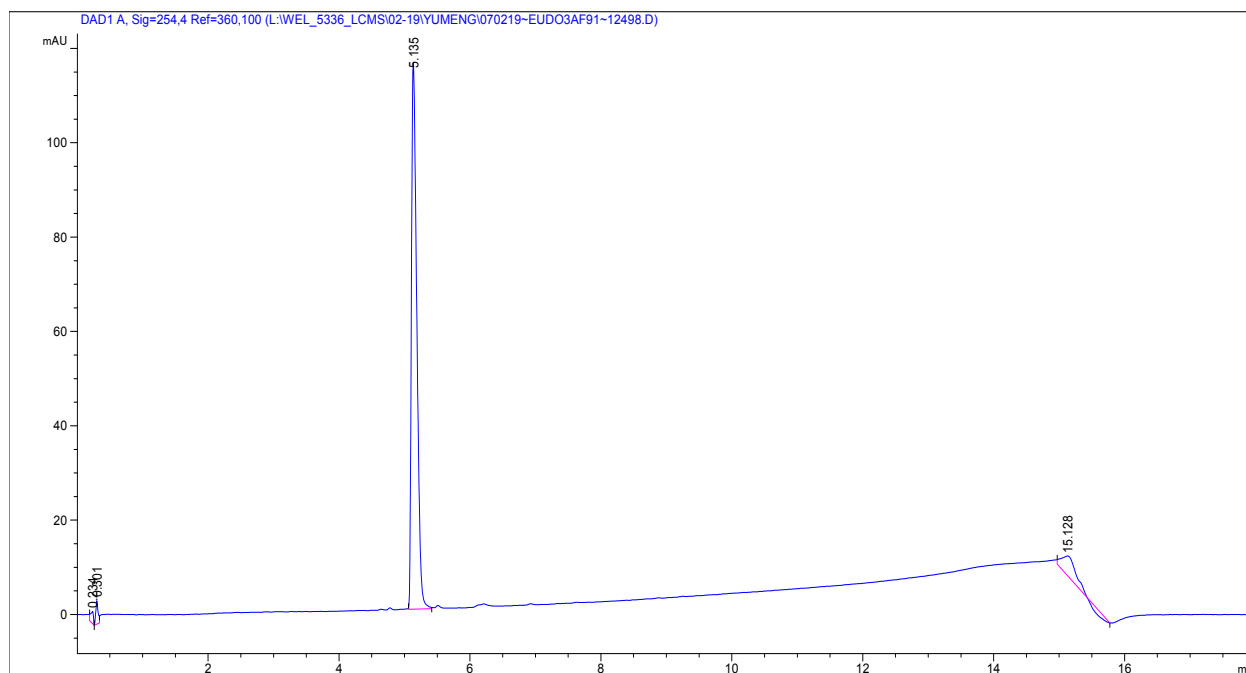
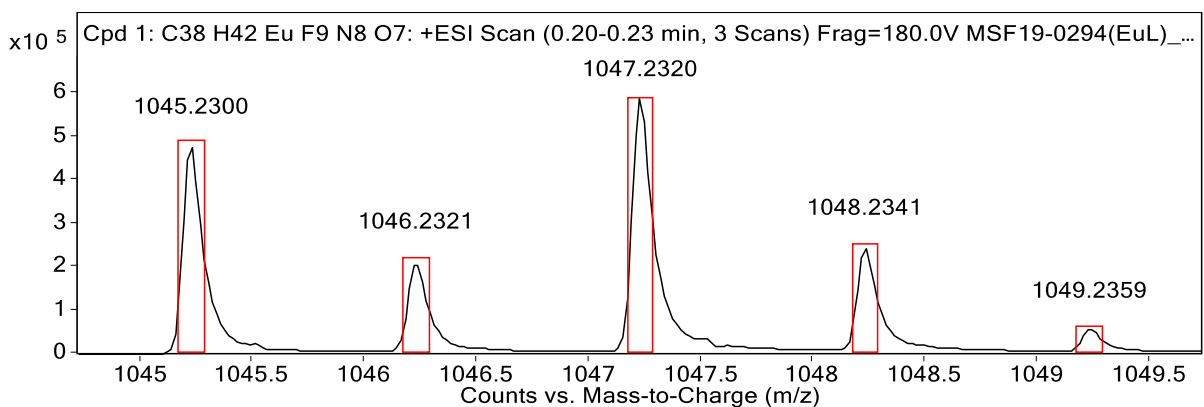


Figure S5. HPLC trace of **Eu-PFZ-1** at 254 nm detection.



MS Spectrum Peak List

Obs. m/z	Calc. m/z	Charge	Abundance	Formula	Ion Species	Tgt Mass Error (ppm)
1045.2300	1045.2304	1	476034	C38H42EuF9N8O7	(M+H)+	0.38
1046.2321	1046.2334	1	210903	C38H42EuF9N8O7	(M+H)+	1.25
1047.2320	1047.2322	1	588396	C38H42EuF9N8O7	(M+H)+	0.21
1048.2341	1048.2349	1	242789	C38H42EuF9N8O7	(M+H)+	0.8
1049.2359	1049.2376	1	51442	C38H42EuF9N8O7	(M+H)+	1.61
1050.2369	1050.2402	1	9511	C38H42EuF9N8O7	(M+H)+	3.11
1051.2362	1051.2428	1	1986	C38H42EuF9N8O7	(M+H)+	6.29

--- End Of Report ---

Figure S6. High resolution mass spectrum of **Eu-PFZ-1**.

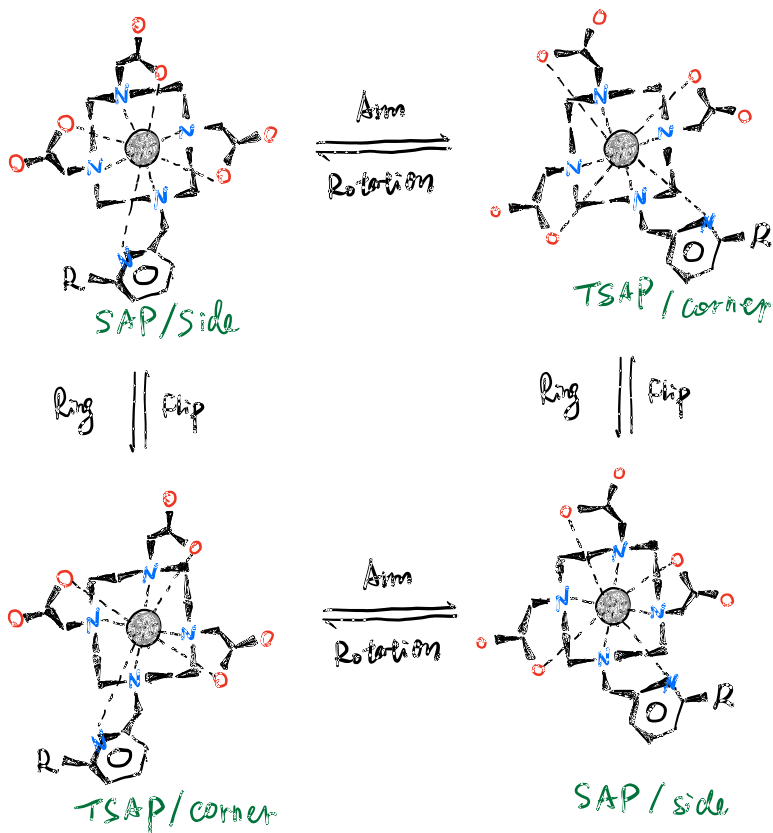


Figure S7. Illustration of structural isomerization due to ring flips and side arm rotations.

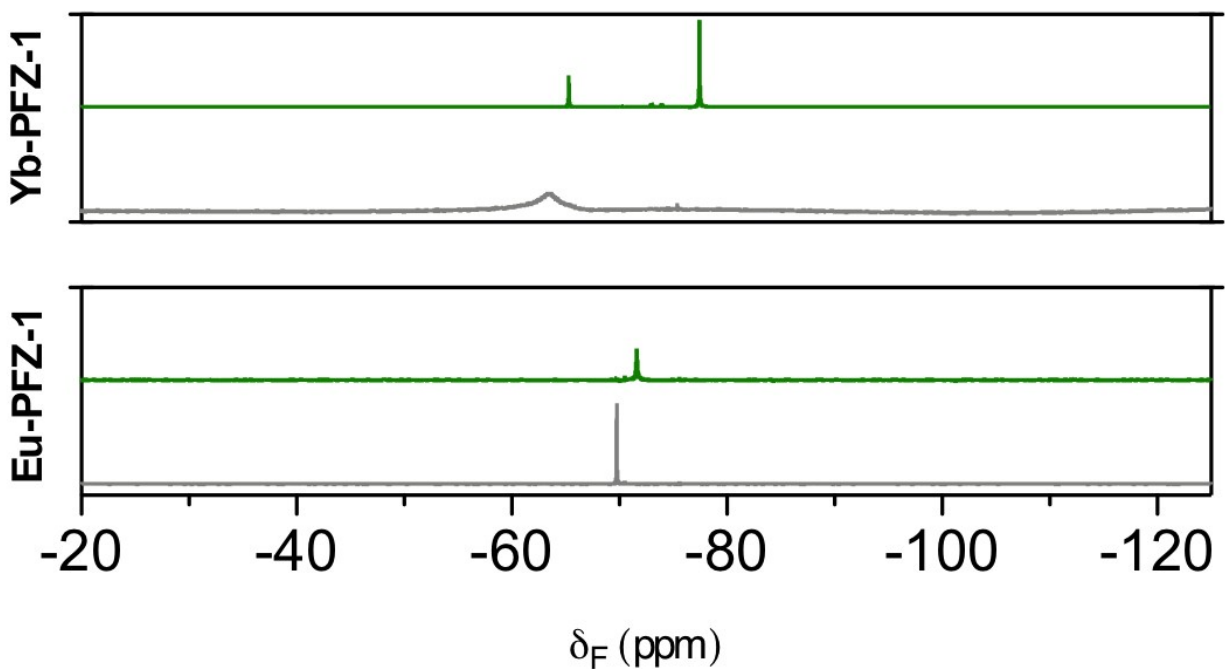


Figure S8. ^{19}F NMR spectra of 2 mM **Yb-PFZ-1** and **Eu-PFZ-1** in 50 mM HEPES buffer (0.1 M KNO_3 , pH 7.4) and in the presence of 1.0 equiv of $\text{Zn}(\text{II})$, acquired at 25 $^{\circ}\text{C}$, 376.5 MHz.

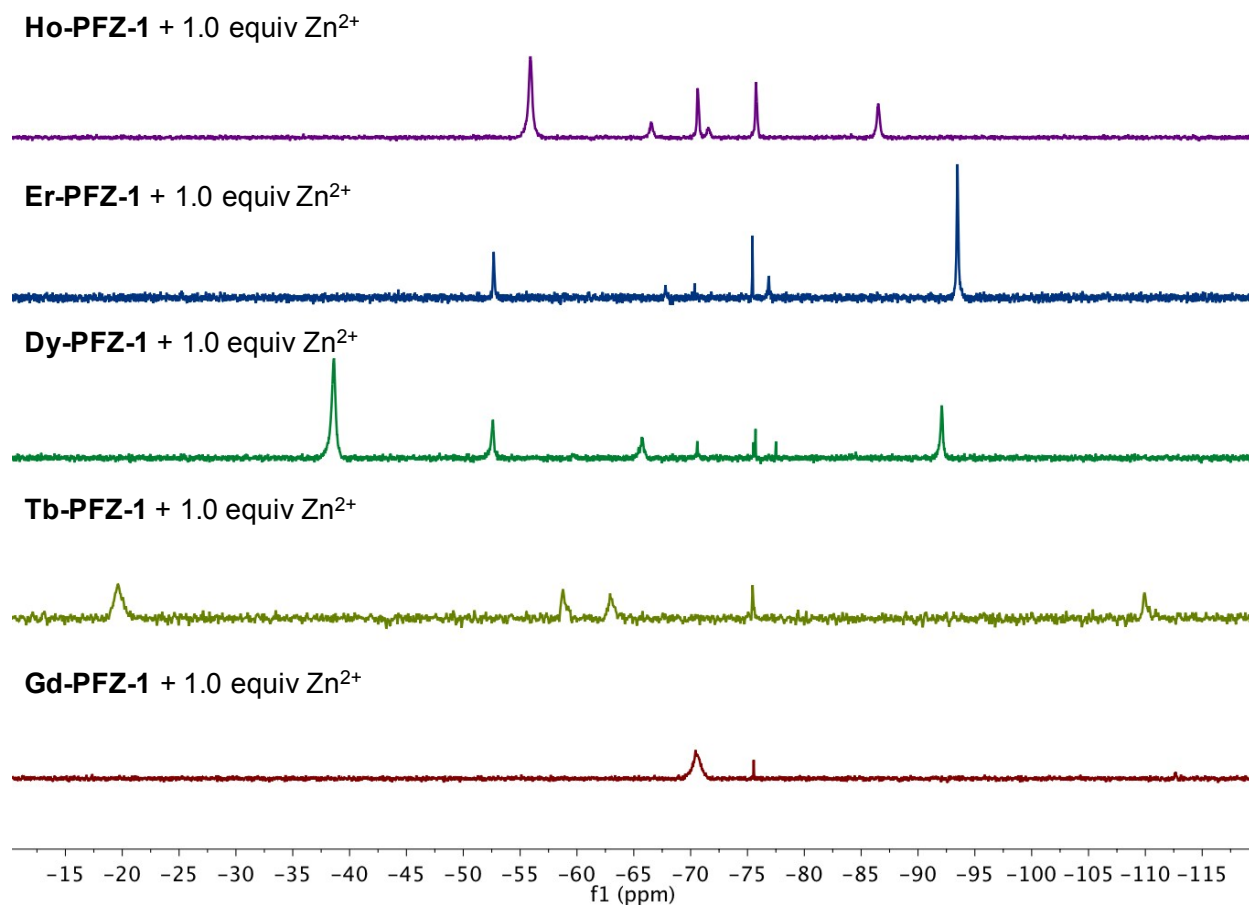


Figure S9. ^{19}F NMR spectra of 2 mM **Gd-PFZ-1**, **Tb-PFZ-1**, **Dy-PFZ-1**, **Er-PFZ-1**, and **Ho-PFZ-1** in 50 mM HEPES buffer (0.1 M KNO_3 , pH 7.4) after adding 1 equiv. Zn^{2+} . Complexes were generated *in situ* by mixing equimolar amount of ligand and lanthanide ions. Note that in the absence of Zn^{2+} , no ^{19}F signal is observed for any of these complexes and thus the spectra are not shown. For Ho^{3+} , Dy^{3+} , Tb^{3+} , and Gd^{3+} , much broader ^{19}F signals were observed after binding Zn^{2+} compared to Tm^{3+} . Though Er^{3+} gave relatively sharp ^{19}F signals, higher percentage of minor isomers were found compared to Tm^{3+} (The Er^{3+} complex also suffers from poor solubility).

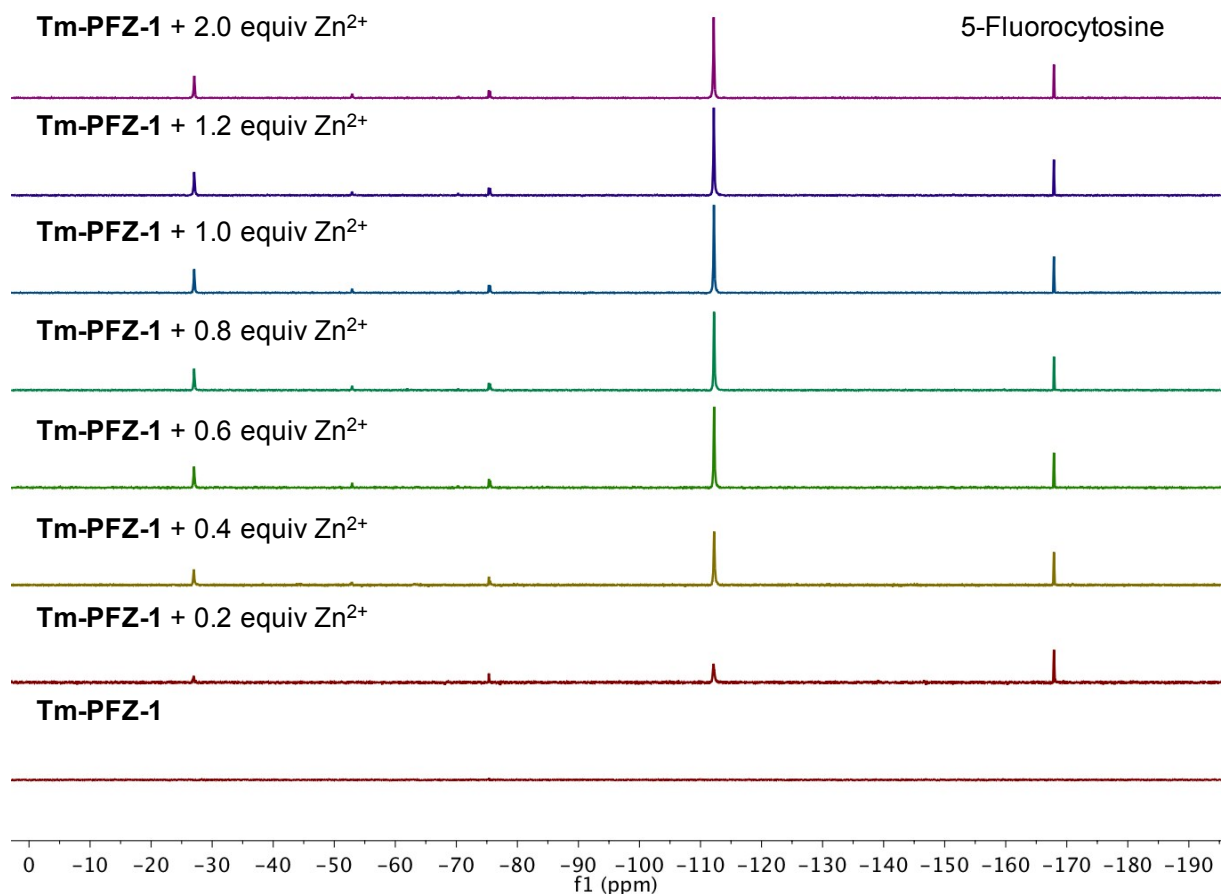


Figure S10. ^{19}F NMR spectra of 2 mM **Tm-PFZ-1** in 50 mM HEPES buffer (0.1 M KNO_3 , pH 7.4) in presence of 0-2.0 equiv of Zn^{2+} . 5-Fluorocytosine was used as an internal ^{19}F standard.

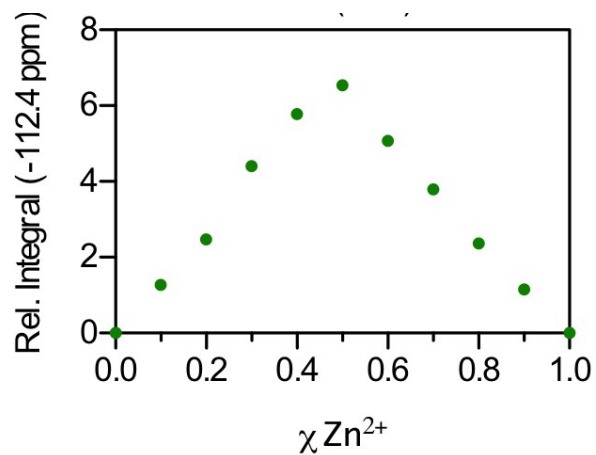


Figure S11. Job's plot of **Tm-PFZ-1** with $\text{Zn}(\text{II})$ following integration of the -112.4 ppm resonance.

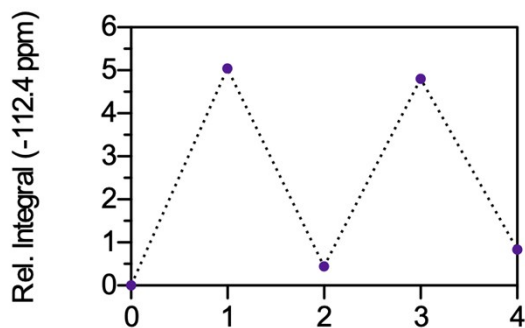
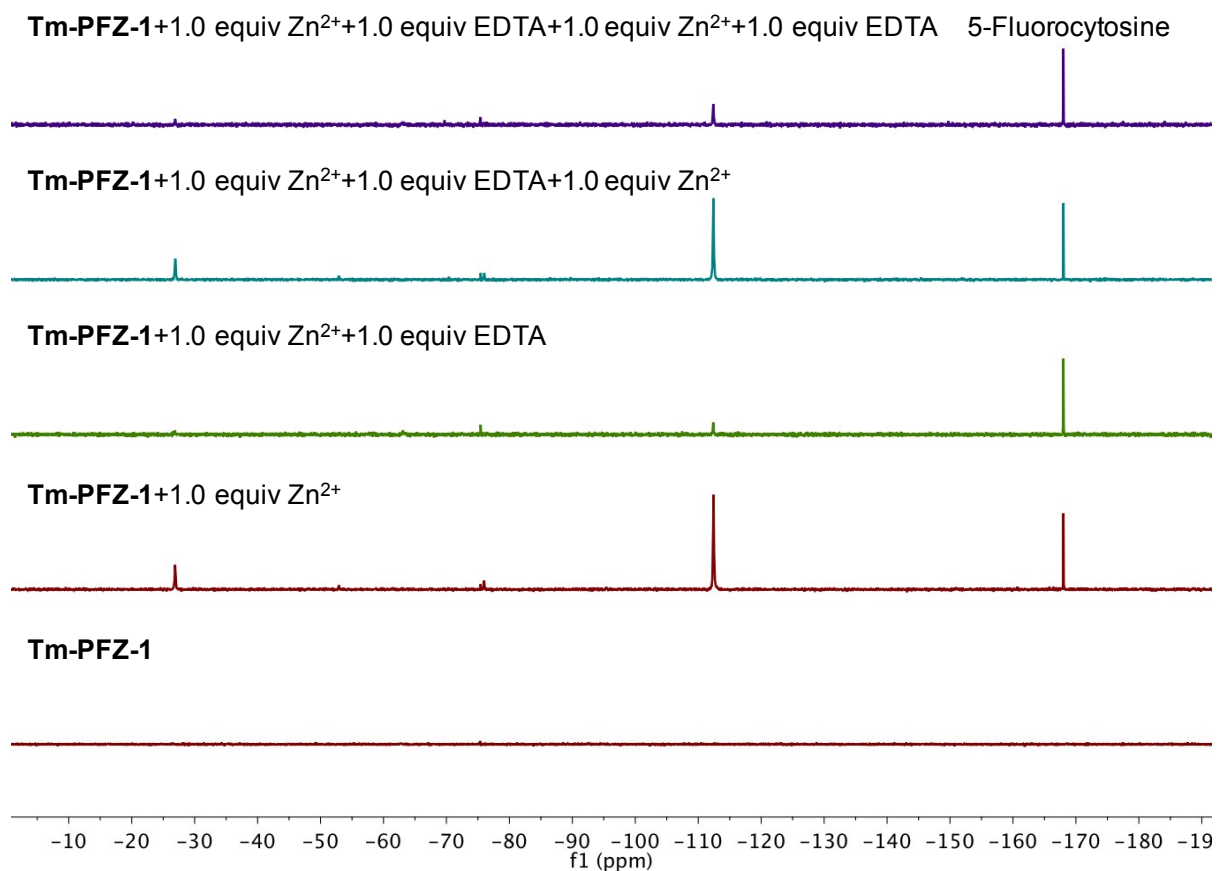


Figure S12. ¹⁹F NMR spectra after repetitive addition of 1 mM Zn²⁺ and 1 mM EDTA to 1 mM **Tm-PFZ-1** in 50 mM HEPES buffer (0.1 M KNO₃, pH 7.4). 5-Fluorocytosine was used as an internal ¹⁹F standard. Graph below shows the integral change at -112.4 ppm during the cycles.

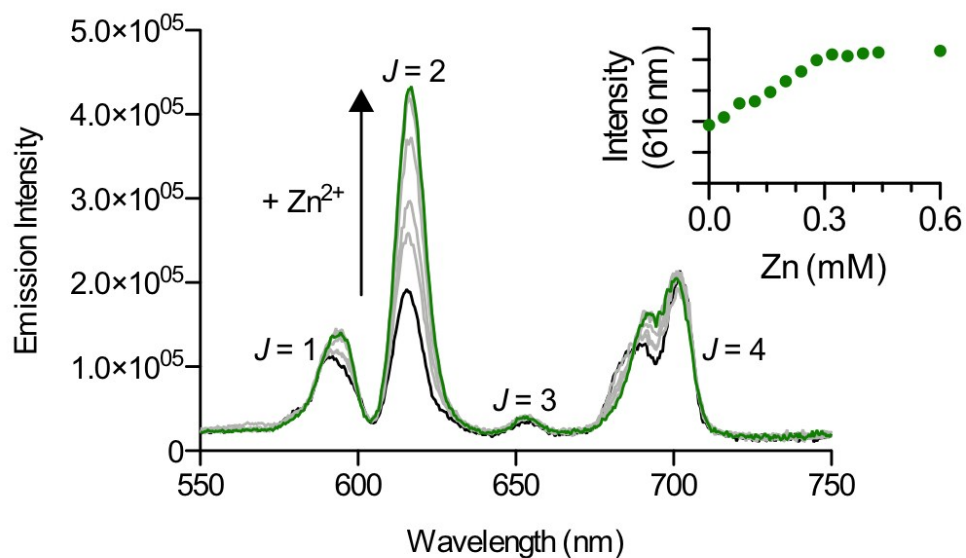


Figure S13. Emission spectra ($\lambda_{\text{ex}} = 265 \text{ nm}$) of **Eu-PFZ-1** (0.3 mM) in the presence of various concentrations of Zn(II): 0-0.6 mM. These spectra were measured in 50 mM HEPES buffer (pH=7.4, 0.1 M KNO_3). The inset shows the changes in the luminescence intensity at $\lambda = 616 \text{ nm}$. The bands arise from $^5\text{D}_0 \rightarrow ^7\text{F}_j$ transitions; the J values of the bands are labeled.

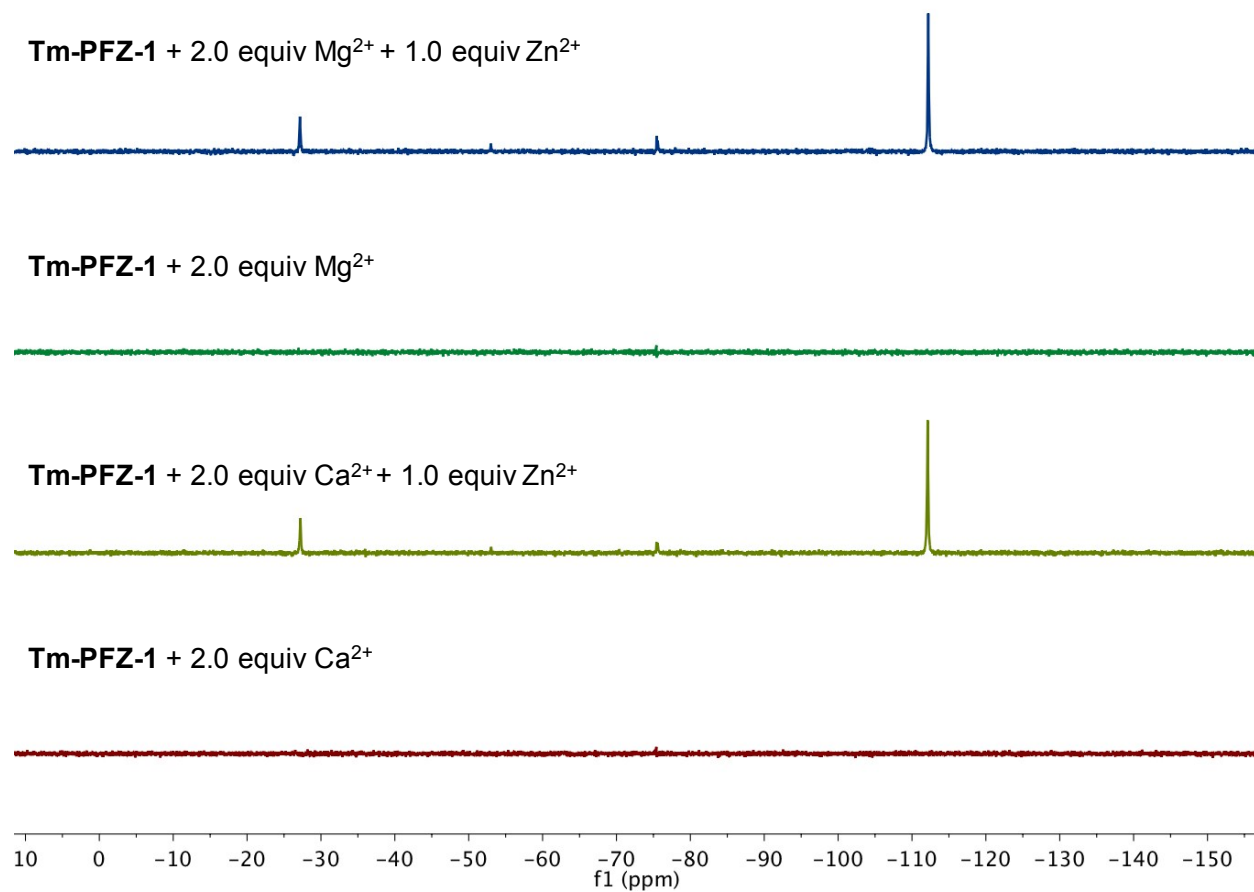


Figure S14. ^{19}F NMR spectra of 1 mM **Tm-PFZ-1** in 50 mM HEPES buffer (0.1 M KNO_3 , pH 7.4) in presence of 2 mM $\text{Ca}^{2+}/\text{Mg}^{2+}$ with or without 1 mM of Zn^{2+} .

Tm-PFZ-1 + 1.0 equiv Cu²⁺

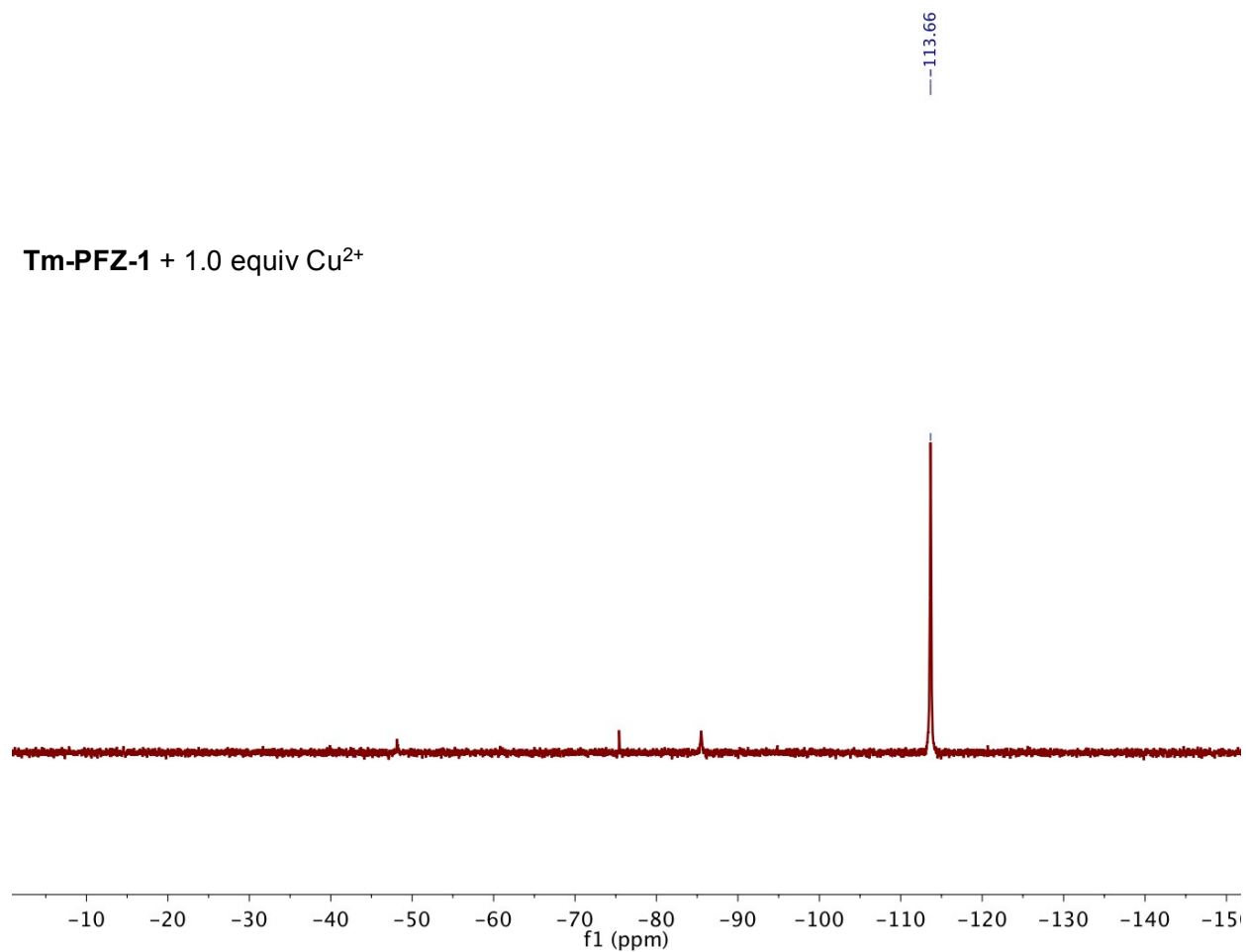


Figure S15. ¹⁹F NMR spectrum of 1 mM **Tm-PFZ-1** in 50 mM HEPES buffer (0.1 M KNO₃, pH 7.4) in presence of 1 mM of Cu²⁺.

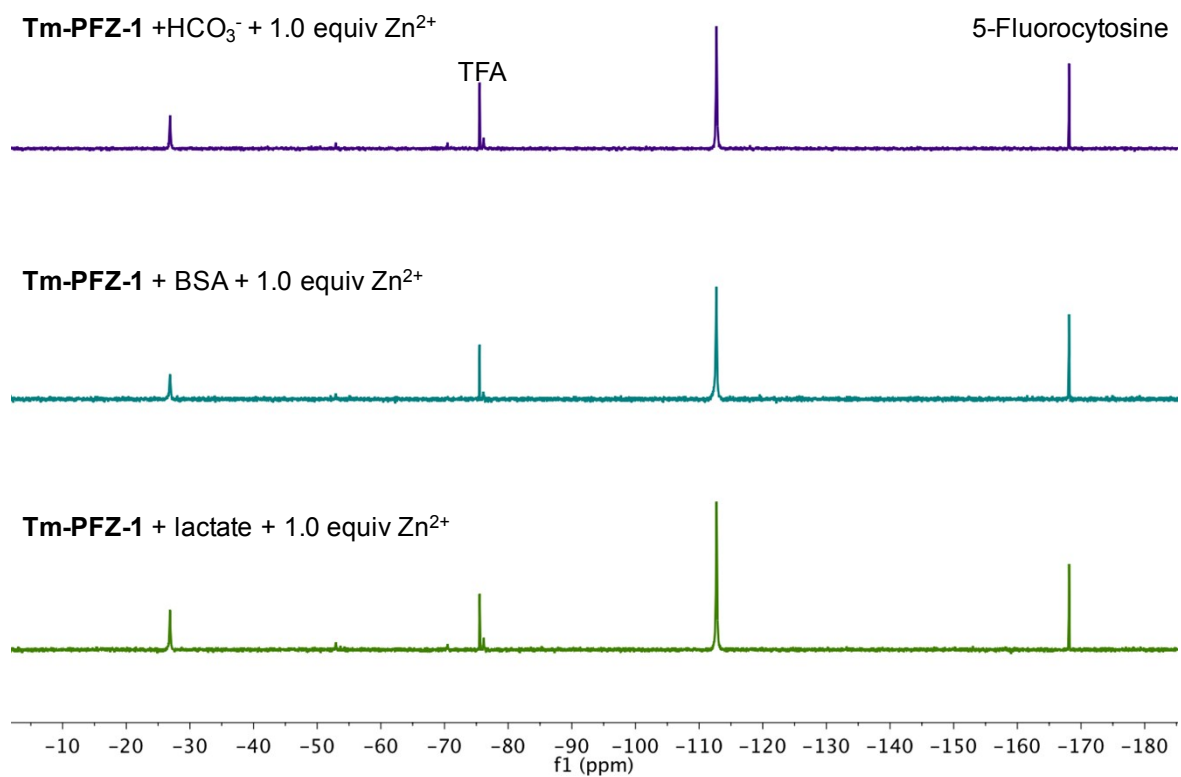


Figure S16. ¹⁹F NMR spectra of 1 mM **Tm-PFZ-1** in 50 mM HEPES buffer (0.1 M KNO₃, pH 7.4) in presence of 2 mM lactate, 10 mM HCO₃⁻ or 5 mg/mL (BSA) and 1 mM Zn²⁺. No ¹⁹F NMR signal was observed in the presence of lactate HCO₃⁻ or 5 mg/mL alone. Note that slight amount of TFA existed as an impurity. 5-Fluorocytosine was used as an internal ¹⁹F standard.

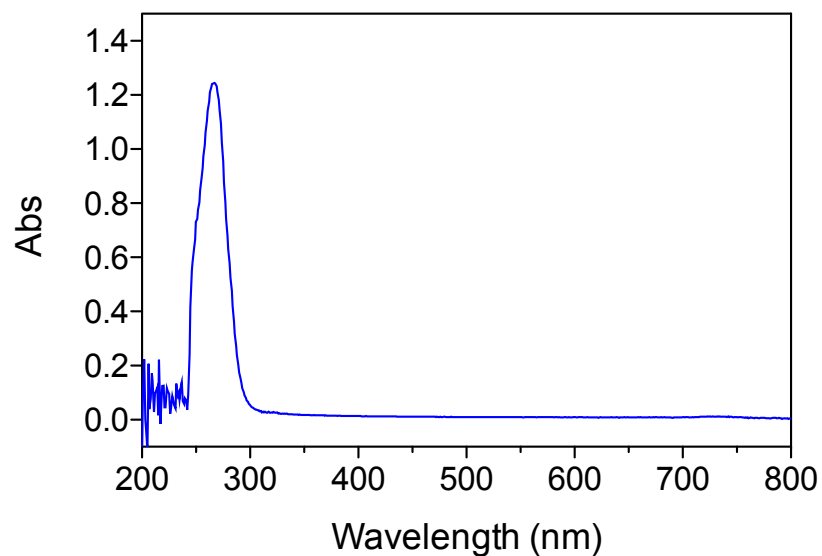


Figure S17. UV-vis spectrum of 0.2 mM **Eu-PFZ-1** in 50 mM HEPES buffer (pH=7.4, 0.1 M KNO₃).

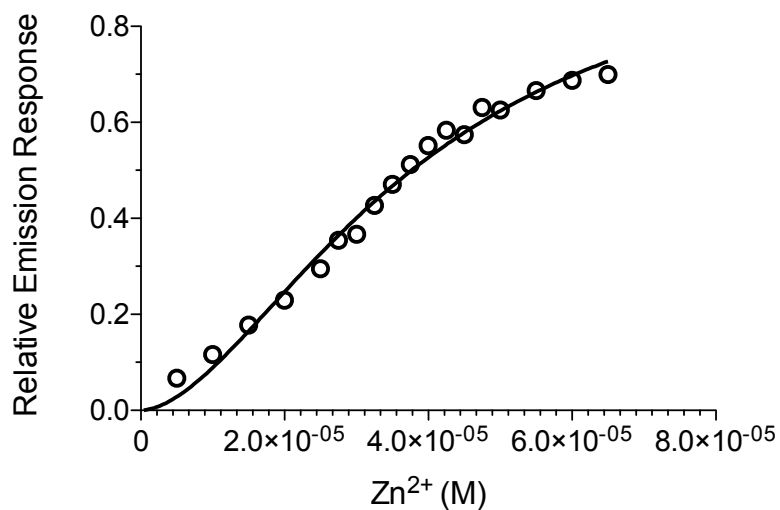


Figure S18. Fitting of luminescence titration data of 50 μM **Eu-PFZ-1** into a 1:1 binding model. Binding constant (K_d) was determined to be $33 \pm 2 \mu\text{M}$.

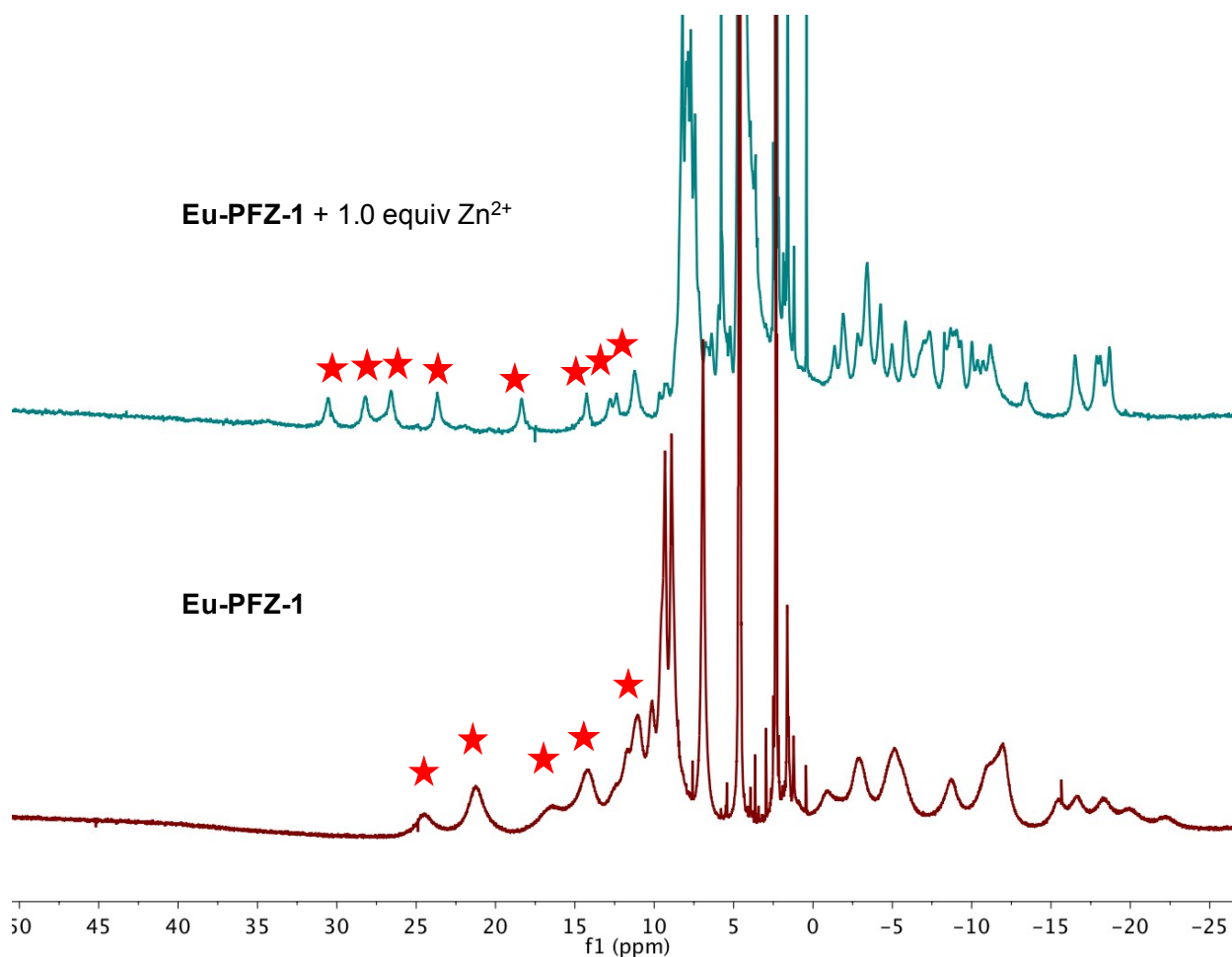


Figure S19. ^1H NMR spectra of 10 mM **Eu-PFZ-1** in D_2O and after adding 10 mM Zn^{2+} .

Table S1. Peak width at half maximum of **Yb-PFZ-1** from 10-85 $^\circ\text{C}$.

	10 $^\circ\text{C}$	25 $^\circ\text{C}$	40 $^\circ\text{C}$	55 $^\circ\text{C}$	70 $^\circ\text{C}$	85 $^\circ\text{C}$
$\Delta\nu_{1/2}$ (Hz)	N/A*	1028.9	887.0	434.2	205.0	98.7
	(63.0 ppm)	(63.7 ppm)	(64.0 ppm)	(64.6 ppm)	(65.3 ppm)	(66.2 ppm)

* The peak was too broad to determine accurately.

Table S2. Peak width at half maximum of **Yb-PFZ-1** after adding 1 equiv. Zn^{2+} from 10-85 $^\circ\text{C}$.

	10 $^\circ\text{C}$	25 $^\circ\text{C}$	40 $^\circ\text{C}$	55 $^\circ\text{C}$	70 $^\circ\text{C}$	85 $^\circ\text{C}$
$\Delta\nu_{1/2}$ (Hz)	11.6	17.7	33.5	76.9	178.2	~276
	(65.5 ppm)	(65.4 ppm)	(65.3 ppm)	(65.3 ppm)	(65.3 ppm)	(65.4 ppm)
$\Delta\nu_{1/2}$ (Hz)	19.9	17.2	21.5	45.8	112.0	189.0
	(78.6 ppm)	(77.4 ppm)	(76.4 ppm)	(75.4 ppm)	(74.6 ppm)	(73.7 ppm)

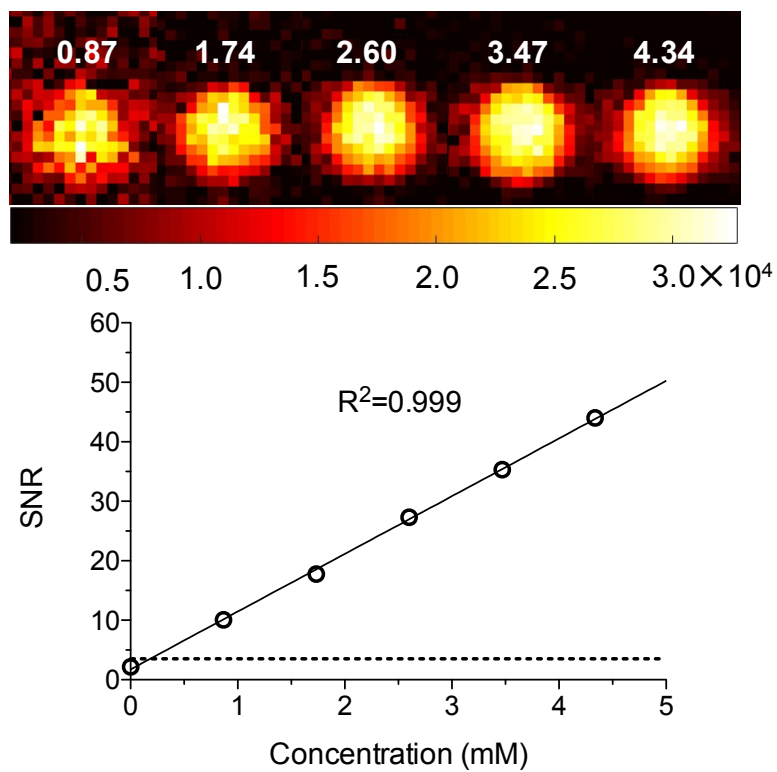


Figure S20. Limit of detection measurement of **Tm-PFZ-1** by ^{19}F MRI. Concentrations of 0.87 – 4.34 mM **Tm-PFZ-1** were used. The images were acquired upon adding 1 equiv. Zn^{2+} . Detailed procedure is provided in the experimental methods.

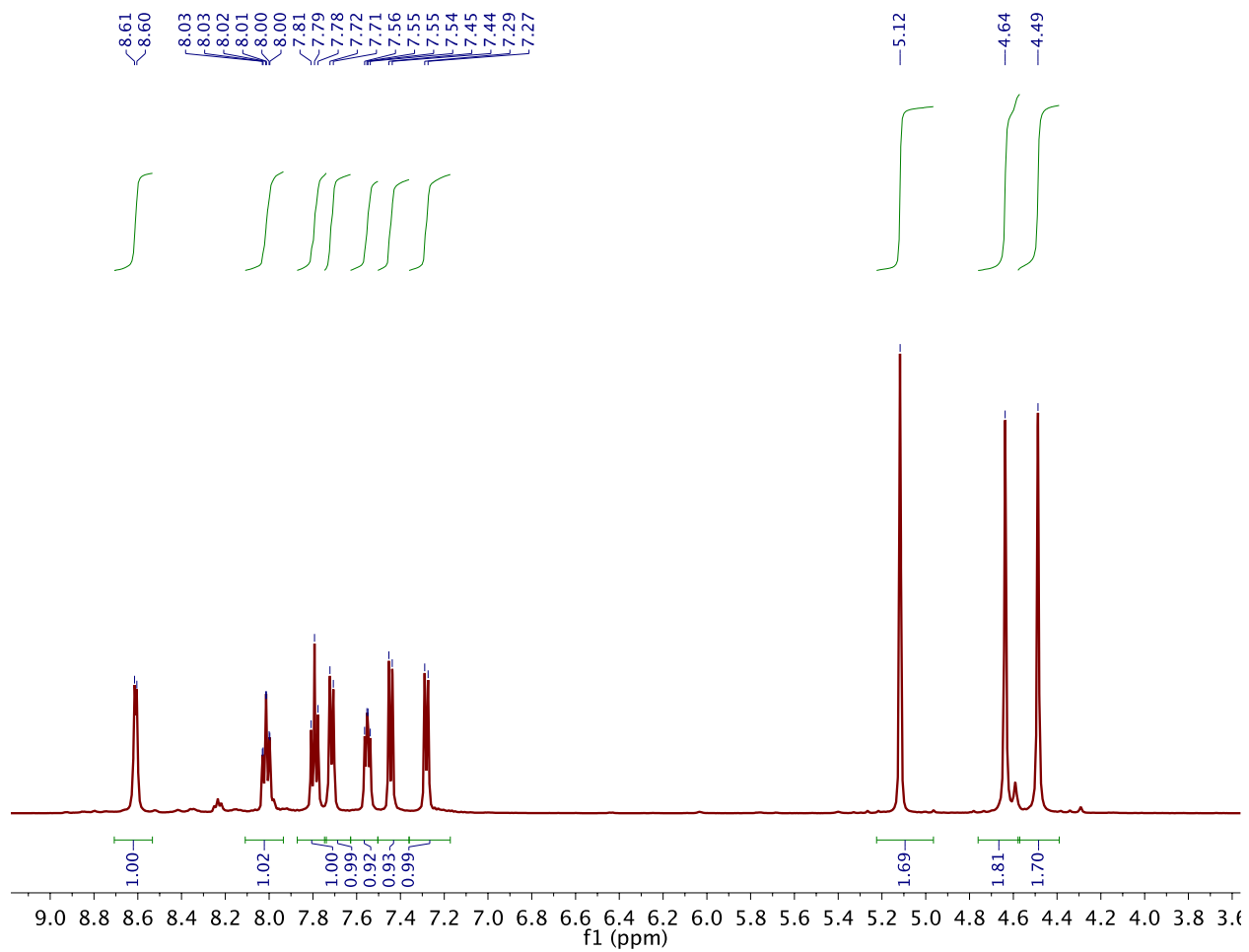


Figure S21. ^1H NMR spectrum of **3** in CDCl_3 .

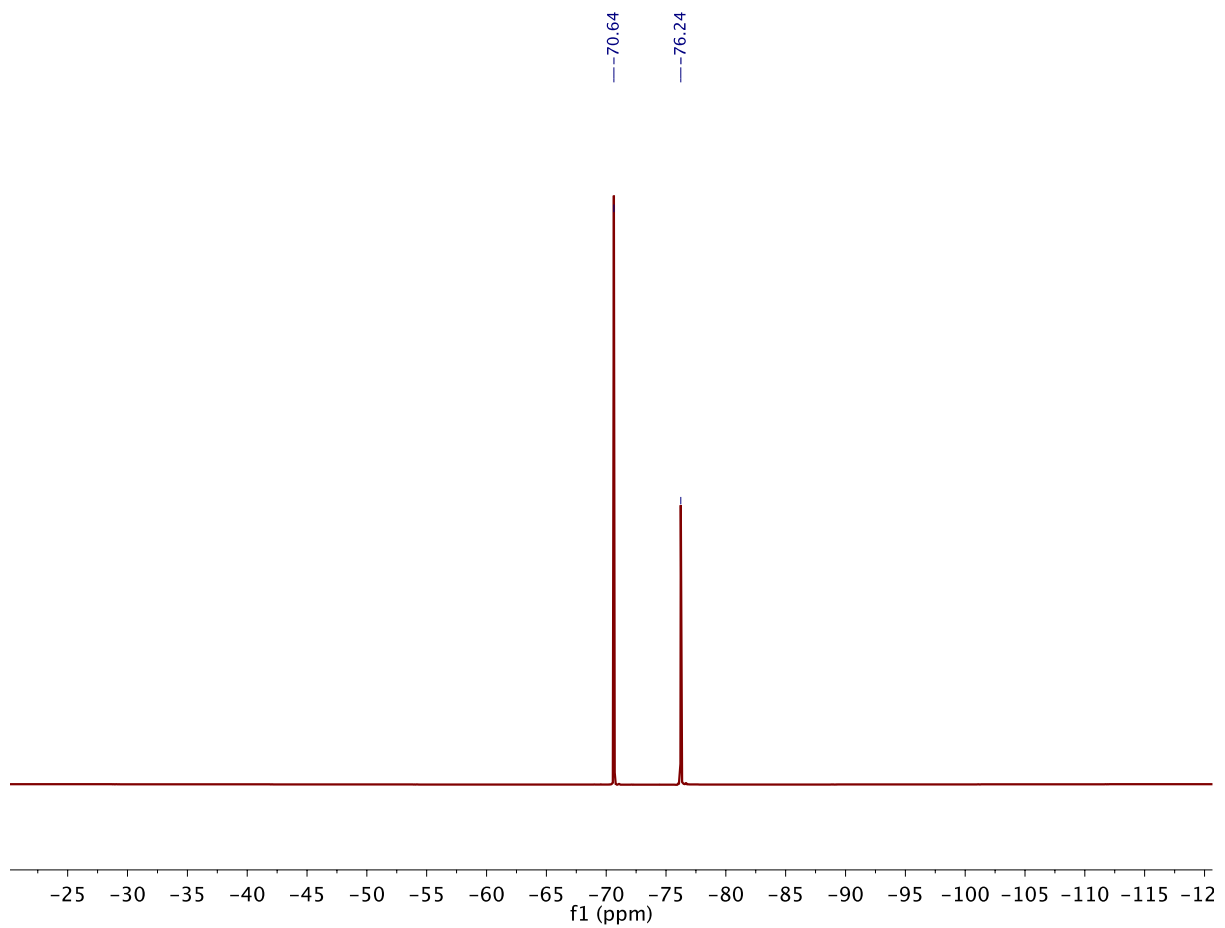


Figure S22. ^{19}F NMR spectrum of **3** in CDCl_3 . Note that the peak at -76.24 ppm is from CF_3COOH .

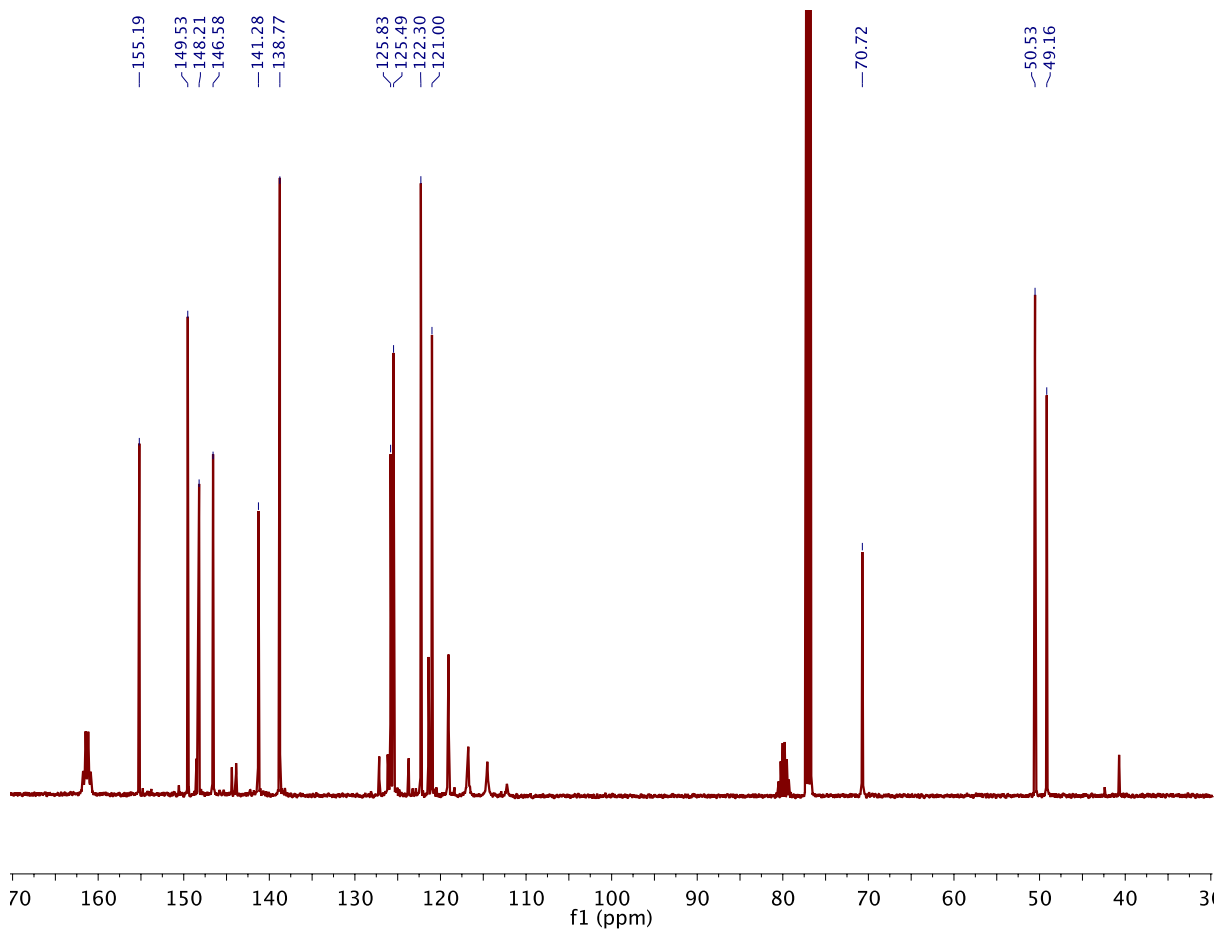


Figure S23. ^{13}C NMR spectrum of **3** in CDCl_3 . Note that the quartets at 162 ppm and 120 ppm are from CF_3COOH .

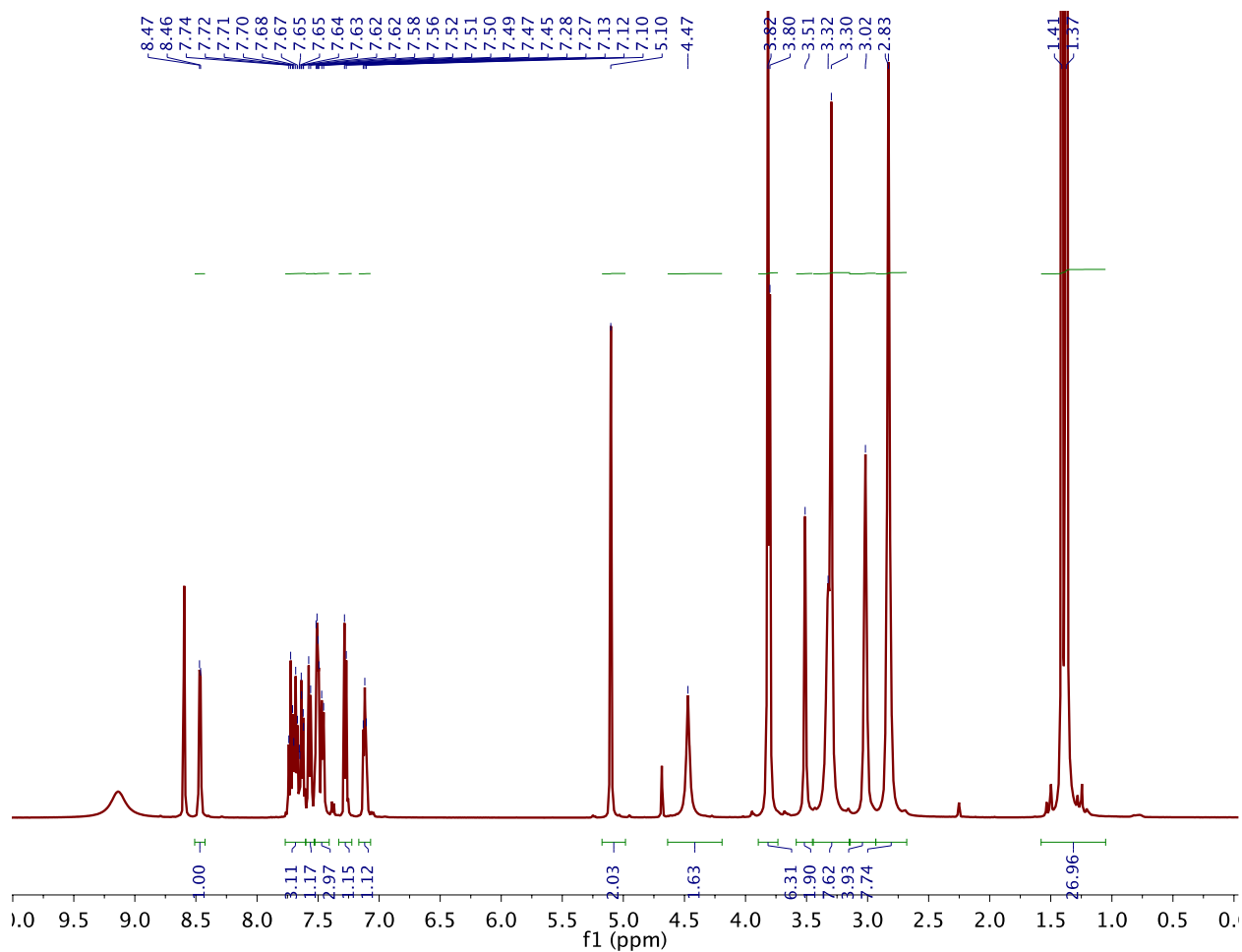


Figure S24. ^1H NMR spectrum of **5** in CDCl_3 . Note that the two peaks at 8.6 ppm and 9.1 ppm belong to HCOOH from reverse phase chromatography.

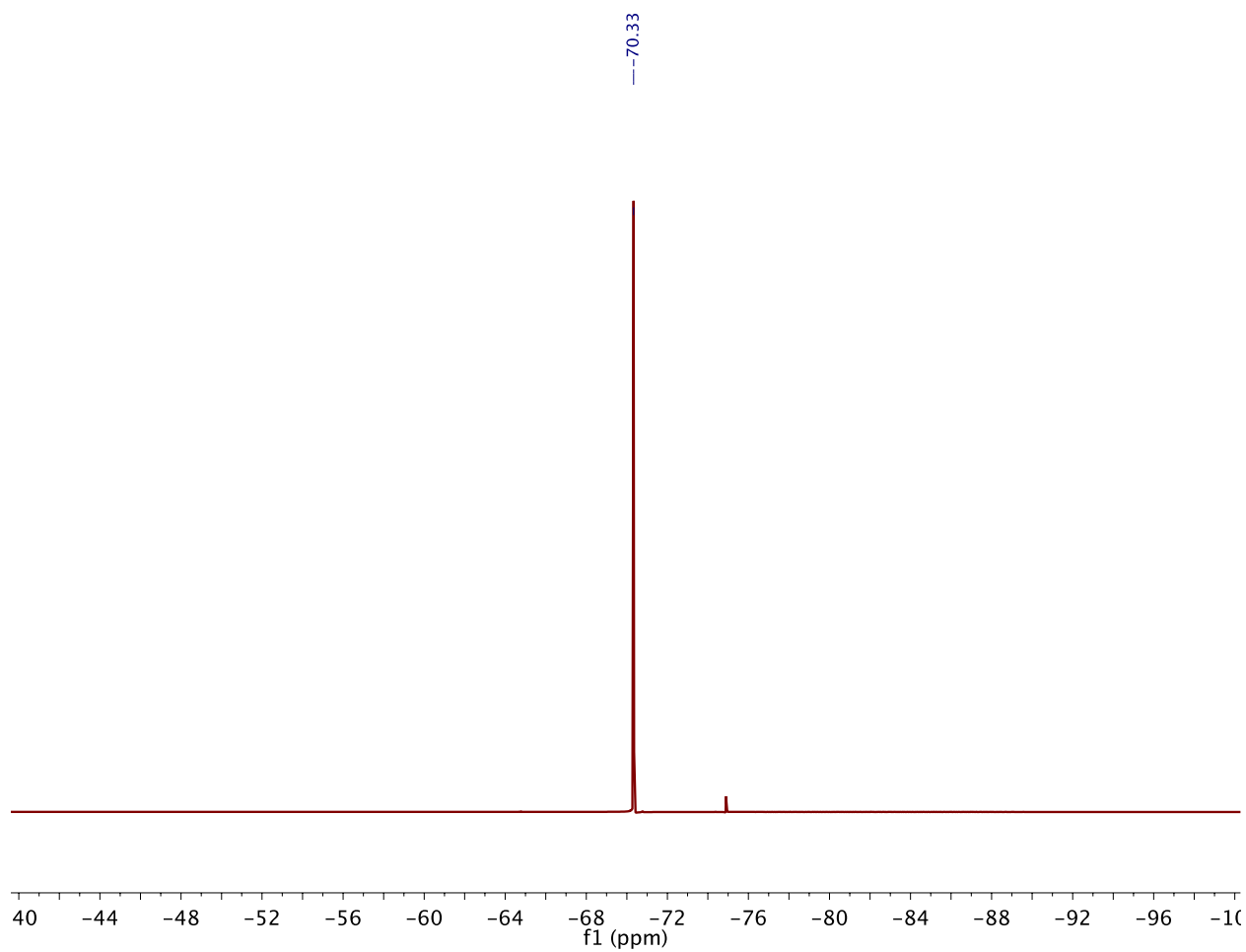


Figure S25. ^{19}F NMR spectrum of **5** in CDCl_3 .

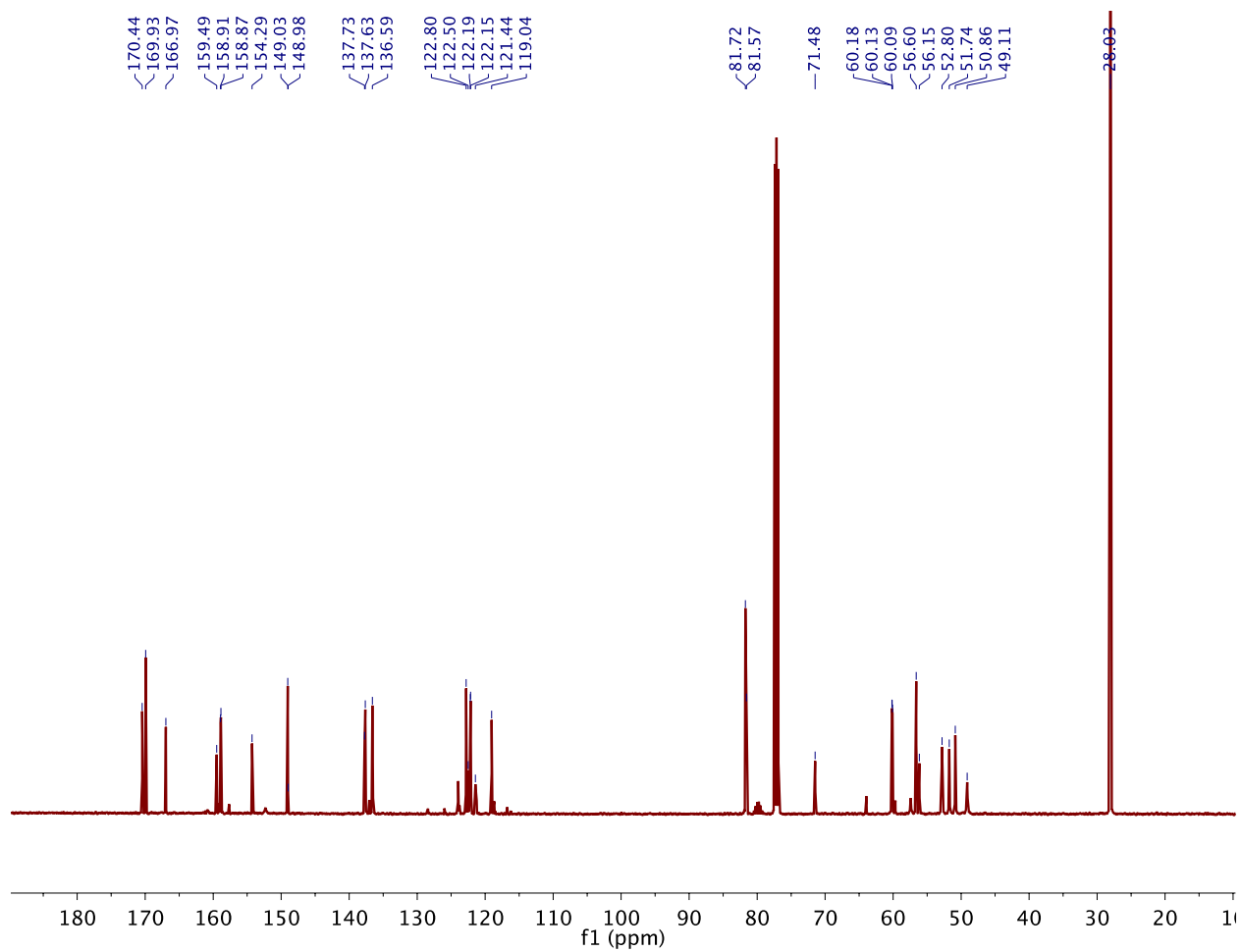


Figure S26. ^{13}C NMR spectrum of **5** in CDCl_3 .

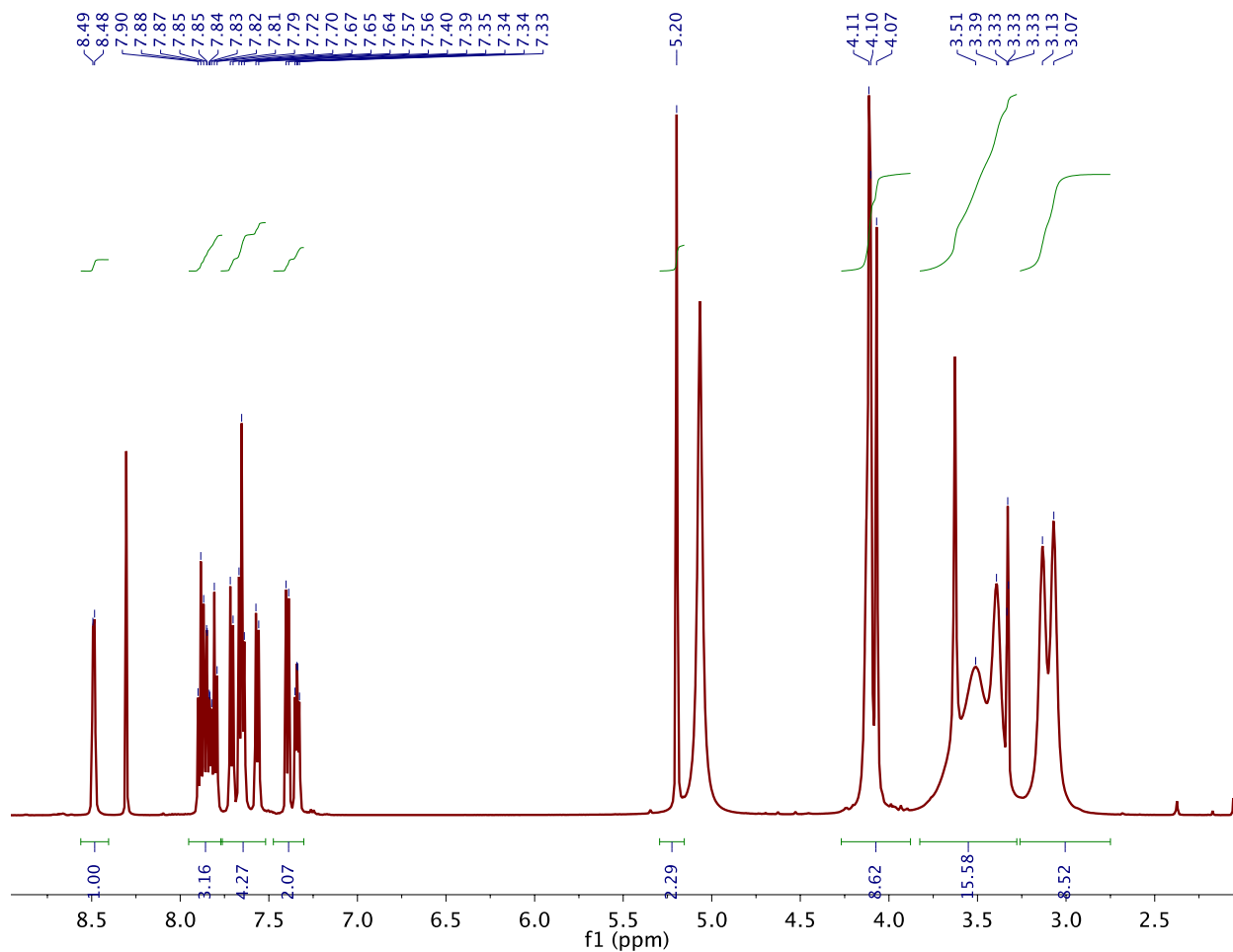


Figure S27. ^1H NMR spectrum of **PFZ-1** ligand in CD_3OD . Note that the peak at 8.3 ppm belongs to HCOOH from reverse phase chromatography. The peaks at 5.1 ppm and 3.6 ppm are CD_3OD solvent peaks.

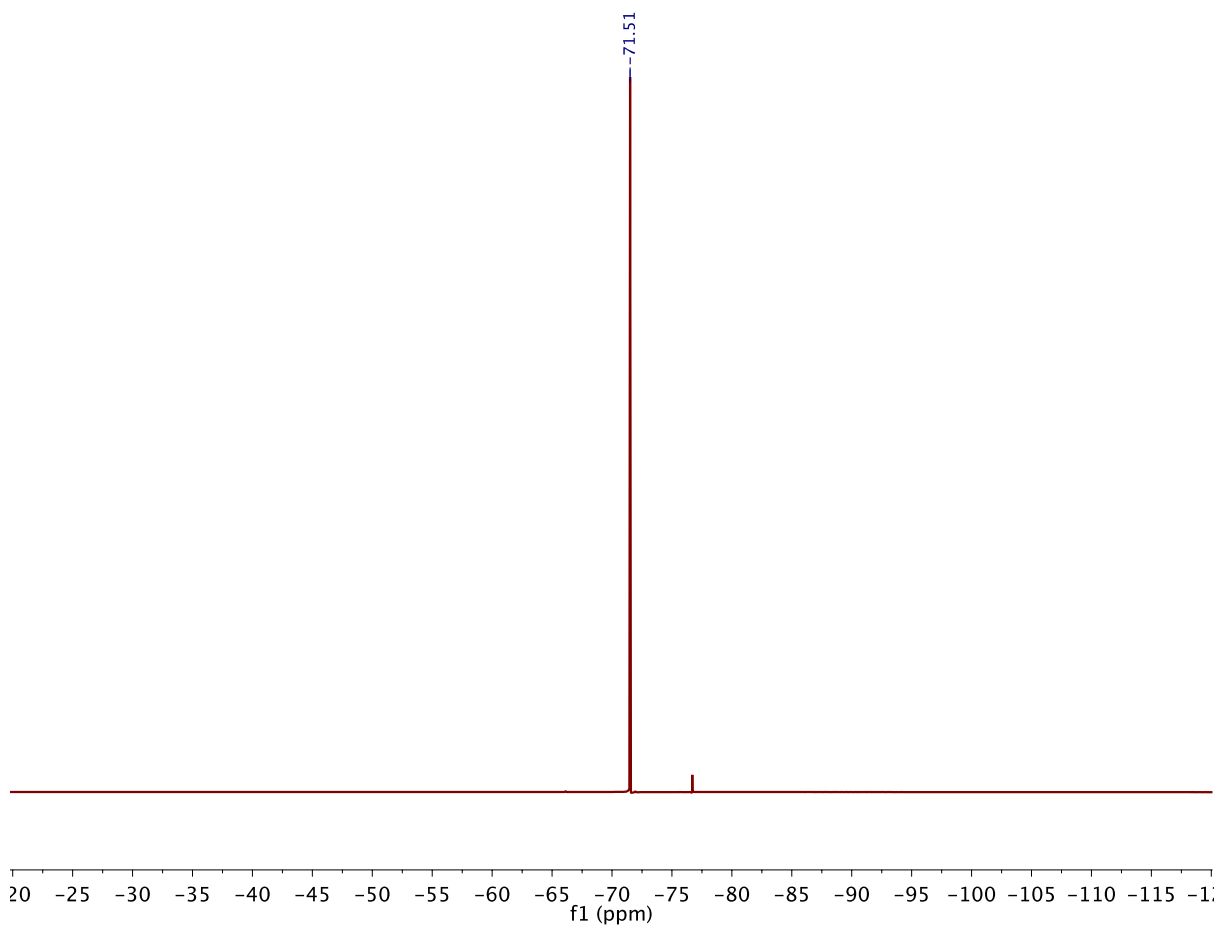


Figure S28. ^{19}F NMR spectrum of **PFZ-1** ligand in CD_3OD .

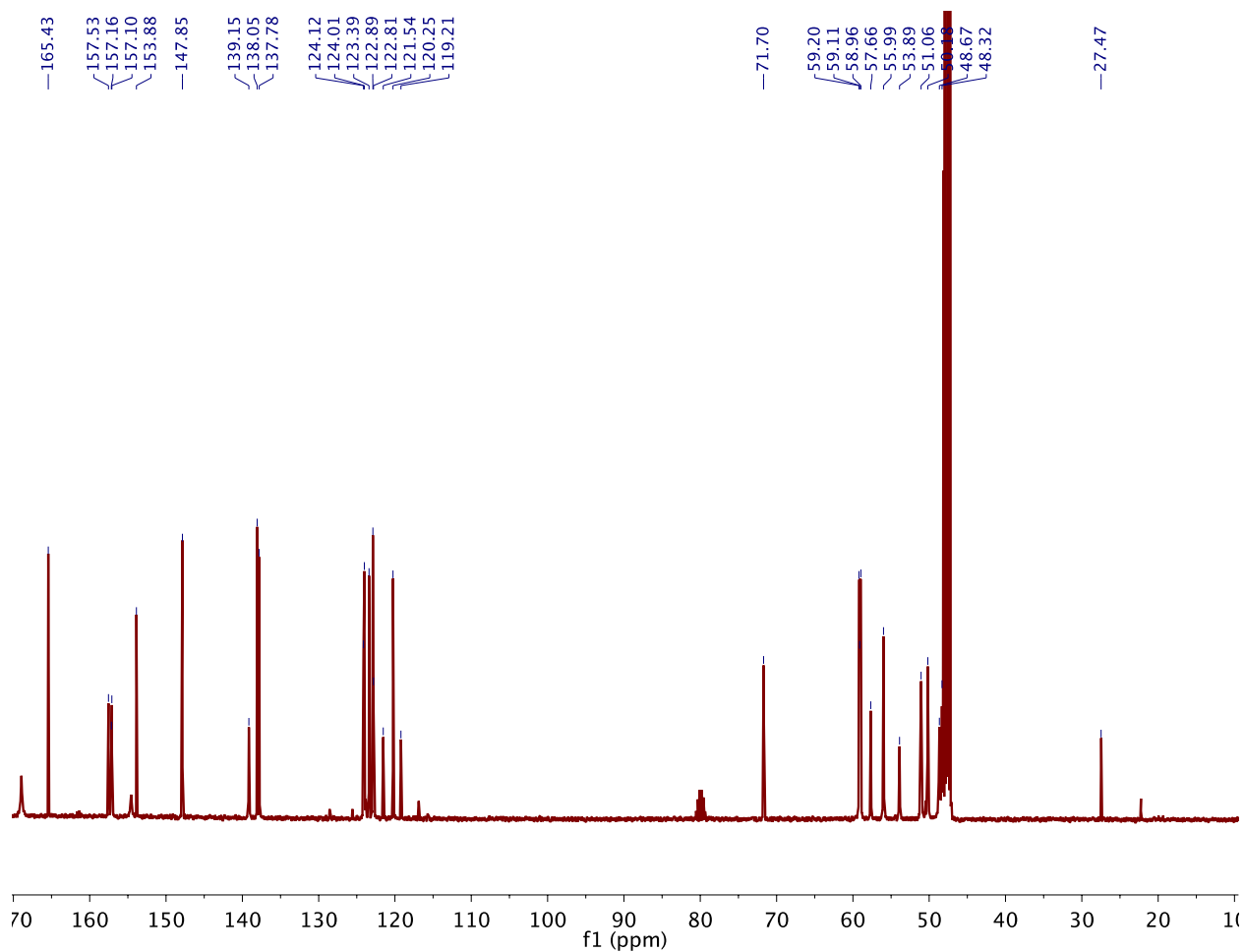


Figure S29. ^{13}C NMR spectrum of **PFZ-1** ligand in CD_3OD .

References

- [1] J. Kim, B. Shin, H. Kim, J. Lee, J. Kang, S. Yanagisawa, T. Ogura, H. Masuda, T. Ozawa, J. Cho, *Inorg. Chem.* **2015**, *54*, 6176–6183.
- [2] D. Xie, S. Kim, V. Kohli, A. Banerjee, M. Yu, J. S. Enriquez, J. J. Luci, E. L. Que, *Inorg. Chem.* **2017**, *56*, 6429–6437.
- [3] M. Andrews, J. E. Jones, L. P. Harding, S. J. A. Pope, *Chem. Commun.* **2011**, *47*, 206–208.
- [4] P. Srivastava, A. K. Tiwari, N. Chadha, K. Chuttani, A. K. Mishra, *Eur J Med Chem* **2013**, *65*, 12–20.